Massachusetts Institute of Technology
Department of Physics

Physics 8.942

Cosmic Microwave Background Anisotropy

1 Introduction

These notes present a simplified computation of cosmic microwave background anisotropy induced by primeval gravitational potential or entropy fluctuations. The basic treatment is equivalent to the calculation of anisotropy on large angular scales presented first by Sachs & Wolfe (1967). The discussion here goes beyond the Sachs-Wolfe treatment to include a discussion of the dominant contributions to anisotropy on small angular scales. The presentation given here is based in part on the PhD thesis of Sergei Bashinsky (Bashinsky 2001) and Bashinsky & Bertschinger (2001, 2002). More elementary treatments of CMB anisotropy are given by Chapter 18 of Peacock and online by Wayne Hu at `http://background.uchicago.edu/`).

We adopt several assumptions in order to simplify the algebra without losing the main physical effects:

1. *Instantaneous recombination.* We assume that, prior to hydrogen recombination at $a = a_r$, photons scatter so frequently with electrons that the photon gas is a perfect gas with spatially-varying energy density ρ_r and fluid three-velocity v^i (orthonormal components of peculiar velocity). This gas is tightly coupled to the "baryons" (electrons plus all ionization states of atomic matter). The gradual decoupling of photons and baryons is approximated by instantaneous decoupling at $a = a_r$. We will indicate how to improve on this treatment by treating the radiation field prior to recombination as an imperfect gas coupled to baryons by Thomson scattering. An accurate treatment of hydrogen and helium recombination is needed in this case. With non-instantaneous recombination, photon polarization must also be considered. We ignore polarization here. The resulting errors are a few percent in rms temperature anisotropy at small angular scales.

2. *No large-scale spatial curvature.* We suppose that the universe is a perturbed Robertson-Walker spacetime. Although the curvature terms (proportional to $1-\Omega$)

will be included in the basic equations, our numerical calculations will not fully include them. This simplifies the harmonic decomposition and is consistent with inflation as the origin of fluctuations. The only important effect we miss is the anisotropy produced by the time-changing gravitational potential at redshift $z < 10$, the integrated Sachs-Wolfe effect.

3. *Adopt a simplified description of matter.* Aside from baryons prior to recombination, we will treat the matter as cold. This is appropriate for CDM and for other types of matter on scales larger than the Jeans length (an excellent approximation for CMB anisotropy). The complex gravitational interaction between photons, neutrinos, and dark matter prior to recombination will be treated in a simplified manner. However, we include correctly, without approximation, a possible nonzero cosmological constant (vacuum energy).

4. *Neglect gravitational radiation.* In the linearized treatment of small-amplitude fluctuations, gravitational radiation is a distinct mode and so its effect on the CMB may be treated as a separate contribution computed independently of the density and entropy fluctuations studied here.

5. *Assume that all perturbations have small (linear) amplitude.* This is valid for "primary" anisotropies but not for "secondary" anisotropies caused by nonlinear structures forming at low redshift. Secondary anisotropies are negligible on angular scales larger than about 10 arcminutes.

The justification for these simplifications is mainly pedagogical, although in general they do not introduce serious errors on angular scales larger than a few degrees of arc. (Gravitational radiation, if present, can contribute significantly to the CMB anisotropy on large angular scales. Curvature also has a significant effect on large scales.) Once the student understands CMB anisotropy in this simplified model, a more realistic treatment can be undertaken (Ma & Bertschinger 1995; Seljak & Zaldarriaga 1996; Zaldarriaga, Seljak, & Bertschinger 1998; Hu et al 1998, and references therein).

Aside from the simplifications given above and some computational approximations stated later, the treatment given herein is rigorous and complete. We will discuss both the "adiabatic" (i.e. isentropic) and "isocurvature" (entropy) modes, the integrated Sachs-Wolfe effect, and both intrinsic and Doppler anisotropies.

The computation of microwave background anisotropy has several ingredients. The rest of these notes give a systematic presentation of these ingredients. In Section 2 we present the Einstein equations for a perturbed Robertson-Walker spacetime. In Section 3 we derive and formally integrate the radiative transfer equation for CMB anisotropy. Section 4 gives a physical interpretation of the primary contributions to CMB anisotropy. These contributions cannot be calculated until the evolution of metric, matter, and radiation perturbations is given, as they provide the source terms for CMB anisotropy. Section

5 presents a simplified set of evolution equations. Section 6 solves these equations on large scales to derive the famous Sachs-Wolfe formula. Section 7 presents a real-space Green's function approach to solving and understanding the small-scale behavior, especially the acoustic peaks. Section 8 shows how to compute the angular power spectrum from the solution of the radiative transfer equation. Numerical results are presented in Section 9.

2 Perturbed Robertson-Walker Spacetimes

This section summarizes the elementary treatment of a weakly perturbed Robertson-Walker spacetime.

We write the spacetime line element as

$$ds^2 = a^2(\tau)\left[-(1+2\phi)d\tau^2 + (1-2\psi)dl^2\right] \tag{1}$$

where dl^2 is the usual spatial line element in comoving coordinates (e.g. $dl^2 = d\chi^2 + r^2 d\Omega^2$, or $dl^2 = dx^2 + dy^2 + dz^2$ in Cartesian coordinates if the background space is flat). The metric perturbations are characterized by two functions $\phi(x^i, \tau)$ and $\psi(x^i, \tau)$ which we assume are small (we neglect all terms quadratic in these fields).

Equation (1) is a cosmological version of the standard weak-field metric used in linearized general relativity. It ignores gravitomagnetism (present in a g_{0i} metric term) and gravitational radiation (present in a transverse-traceless strain tensor h_{ij} added to the spatial metric). Note that the Newtonian limit follows from equation (1) when $\dot{a} = 0$ and $\phi = \psi$. Dots denote derivatives with respect to conformal time τ, while gradient symbols (e.g. ∇_i) represent gradients (covariant derivatives) with respect to the comoving spatial coordinates using the unperturbed 3-metric of dl^2. In a flat background with Cartesian coordinates, $\nabla_i = \partial_i$.

As in the standard treatment of linearized general relativity, we describe spacetime by perturbations added to a background model. The coordinate-freedom allows us many ways to do this for a given set of physical perturbations. We will not discuss this gauge-fixing problem in these notes. Bertschinger (1996) discusses this issue in detail. Equation (1) conveniently avoids gauge artifacts and enables us to focus on the physics.

In the following, we often speak of "fundamental" (or "comoving") observers by which we mean observers at fixed x^i. The 4-velocity of a fundamental observer is $\vec{V} = a^{-1}(1-\phi)\vec{e}_\tau$. In general, fundamental observers are not freely-falling (as one can see from the geodesic equation for $dV^i/d\lambda$), nor do they correspond to the rest frame of a galaxy or to the frame in which the CMB dipole anisotropy vanishes. (See Peacock section 9.4 for a discussion of the dipole anisotropy caused by the Doppler effect.) However, they define a very convenient set of local rest frames in which to project tensor components.

As usual, we construct an orthonormal basis (a tetrad) at each spacetime point with $\vec{e}_{\hat{0}} = \vec{V}$ and with the spatial axes being parallel to the coordinate axes assuming that we use orthogonal coordinates for the background Robertson-Walker spacetime. (The spatial curvature perturbation $1 - \psi$ does not affect the orthogonality of the comoving coordinate axes as it is a conformal factor for dl^2.) Energy, momentum, three-velocity (i.e. proper peculiar velocity), energy density, entropy density, etc. all have the same meanings as in special relativity when obtained from tensor components with a fundamental observer's orthonormal basis. Note that there is such an observer at every point in space; we don't (yet) preferentially single out the observer at $\chi = 0$.

In the absence of anisotropic, relativistic stresses (produced mainly by neutrinos in the early universe), $\phi = \psi$ and the spacetime metric perturbations are described by a single Newtonian-like gravitational potential. In this case, equation (1) is identical to the usual weak-field metric in the Newtonian limit aside from the conformal factor $a^2(\tau)$ arising from cosmic expansion. In the following, we will distinguish the two metric functions in order to keep track of which physical effects arise from the gravitational redshift part of the metric (ϕ) and which arise from the spatial curvature part (ψ).

The unperturbed, or background, density $\bar{\rho}(t)$ obeys the Friedmann equation:

$$\left(\frac{d\ln a}{d\tau}\right)^2 = \frac{8\pi}{3} G\bar{\rho}a^2 - K \ . \tag{2}$$

Note that because $\bar{\rho} \propto a^{-3}$ in the matter-dominated era and $\bar{\rho} \propto a^{-4}$ in the radiation-dominated era, the curvature term is negligible at high redshift. However, spatial curvature affects the geometry at low redshift and does have an effect on CMB anisotropy.

For later use, we provide the solution to equation (2) for a model consisting of only matter (with present density parameter Ω_m) and radiation (whose energy density equals that of matter at $a = a_{\rm eq} = 2.41 \times 10^4\, \Omega_m h^2$):

$$\frac{a(\tau)}{a_{\rm eq}} = \left(\frac{\tau}{\tau_e}\right) + \frac{1}{4}\left(\frac{\tau}{\tau_e}\right)^2 \ , \quad \text{where} \quad H_0\tau_e \equiv \left(\frac{a_{\rm eq}}{\Omega_m}\right)^{1/2} \ . \tag{3}$$

Note that $a = a_{\rm eq}$ at $\tau = 2(\sqrt{2} - 1)\tau_e$. For $\Omega_m = 0.35$ and $h = 0.7$, $a_{\rm eq}^{-1} = 4100$ and $\tau_e = 110$ Mpc. This solution neglects curvature and a cosmological constant but should be accurate to better than 0.1% during recombination.

3 CMB Radiative Transfer

We wish to determine the specific intensity I_ν measured by the observer at $\chi = 0$ and $\tau = \tau_0$ as a function of photon direction and energy. Conceptually, the way we will do it is by tracing photon trajectories back from $\chi = 0$ to recombination at radial coordinate

distance $\chi_{\rm e} = \tau_0 - \tau_{\rm e}$. The subscript "e" stands for *emitter* and reminds us that we are looking at radiation emitted from a photosphere, the edge of the plasma layer that exists for $\chi > \chi_{\rm e}$, i.e. for times $\tau < \tau_e$. We see the CMB as though we live in a transparent spherical cavity of radius $\chi_{\rm e}$ beyond which is a hot glowing plasma. Of course, $\chi_{\rm e}$ really represents a boundary in *time* rather than space; every fundamental observer has a different photosphere.

In the absence of emission, absorption, and scattering, conservation of photons implies that the photon phase space density is conserved along null geodesics. In the language of basic astronomy, $dI_\nu/ds = 0$ where I_ν is the specific intensity and ds measures path length. However, unlike most other astronomical situations, the path length measures not just distance in space; d/ds measures the rate of change in *phase* space. The radiation field varies with time, energy (photon frequency) and photon direction as well as with position in space. We will work out these dependencies to calculate the CMB anisotropy. First, however, we must examine the cosmological radiative transfer equation more closely.

3.1 Derivation of radiative transfer equation

In place of the specific intensity, we use the radiation brightness temperature to characterize the phase space distribution. Let E be the photon energy measured by a fundamental observer and let $n^i = p^i/E$ be a unit vector (with respect to the observer's orthonormal basis) in the direction of photon travel. The brightness temperature $T_{\rm br}(x^i, \tau, E, n^i)$ is defined implicitly through $I_\nu = B_\nu(T_{\rm br})$ where $B_\nu(T)$ is the Planck function and I_ν is the specific intensity measured by the fundamental observer at (x^i, τ).

Because the radiation perturbations are small, we write $T_{\rm br} = a^{-1}T_0(1+\Delta)$ where T_0 is the present unperturbed blackbody temperature and $\Delta^2 \ll 1$. Our Δ coincides with Peacock's $\delta T/T$; most other workers write $\Delta T/T$. Thus, the photon phase space distribution (summed over polarizations) is

$$f(x^i, \tau, E, n^i) = \frac{c^2 I_\nu}{2\pi\hbar^4\nu^3} = f_{\rm P}\left(\frac{aE}{1+\Delta}\right) \ , \quad \text{where} \quad f_{\rm P}(\epsilon) \equiv 2\hbar^{-3}\left[\exp(\epsilon/T_0) - 1\right]^{-1} \ . \tag{4}$$

[The unperturbed temperature T_0 can, in fact, never be measured because we see only the perturbed universe. Separating the radiation field into an unperturbed "background" plus perturbations is really a fiction chosen for the calculational convenience of linear perturbation theory. In practice, T_0 is replaced by the average of the brightness temperature taken over the sky. Anisotropy measurements are made by subtracting pairs of brightness temperatures from different directions in the sky. Uncertainty in T_0 affects only the "monopole" anisotropy, which is unmeasurable and consequently ignored by observers of CMB anisotropy. The same is true of the "dipole" anisotropy, which receives contributions from both the observer's motion and an intrinsic anisotropy due to

a possible large-scale gradient of brightness temperature across our Hubble volume. The choice of rest frame for fundamental observers is arbitrary; in practice it is chosen so that the dipole anisotropy vanishes at the solar system barycenter.]

In general, the brightness temperature is a function of photon energy. However, we will see that for primary CMB anisotropies, the energy-dependence disappears: $\Delta = \Delta(x^i, \tau, n^i)$. That is, in every direction, a fundamental observer finds that the specific intensity is a perfect black-body as a function of photon energy but with the temperature varying with photon direction. A simple example of this behavior is the Doppler anisotropy derived by Peacock in his Section 9.4. However, it holds also for all forms of CMB anisotropy that do not involve large-amplitude perturbations.

Secondary anisotropies induced by nonlinear structures at low redshift often depend on energy (i.e. the spectrum is distorted from blackbody). An example is the Sunyaev-Zel'dovich effect caused by scattering of CMB photons by hot ionized gas in clusters of galaxies. The spectral signature makes it easy to distinguish Sunyaev-Zel'dovich anisotropy from primary CMB anisotropy. These notes consider only the primary anisotropies.

Our goal is to determine $\Delta_0(n^i) = \Delta(\chi = 0, \tau_0, n^i)$, the anisotropy measured by the fundamental observer at the origin. (The anisotropy measured by a *moving* observer at the origin, e.g. one on the Earth, follows by a simple Doppler shift following Peacock eq. 9.62.) We use the fact that the photon phase space density is conserved in the absence of emission, absorption, and scattering. From equation (4), the total change in the phase space density is (assuming $\Delta^2 \ll 1$)

$$\begin{aligned} \frac{df}{d\tau} &= \left(\frac{aE}{1+\Delta}\right) f'_{\rm P}\left(\frac{aE}{1+\Delta}\right)\left[\frac{d\ln(aE)}{d\tau} - \frac{d\Delta}{d\tau}\right] = \left(\frac{df}{d\tau}\right)_{\rm c} , \\ \text{where} \quad \frac{d\Delta}{d\tau} &= \frac{\partial\Delta}{\partial\tau} + \frac{\partial\Delta}{\partial x^i}\frac{dx^i}{d\tau} + \frac{\partial\Delta}{\partial E}\frac{dE}{d\tau} + \frac{\partial\Delta}{\partial n^i}\frac{dn^i}{d\tau} . \end{aligned} \tag{5}$$

We may thus write the radiative transfer equation as

$$\frac{\partial\Delta}{\partial\tau} + \frac{\partial\Delta}{\partial x^i}\frac{dx^i}{d\tau} + \frac{\partial\Delta}{\partial E}\frac{dE}{d\tau} + \frac{\partial\Delta}{\partial n^i}\frac{dn^i}{d\tau} = \frac{d\ln(aE)}{d\tau} + \left(\frac{d\Delta}{d\tau}\right)_{\rm c} \tag{6}$$

where the term with a subscript c accounts for collisions (emission, absorption, and scattering of photons).

We can simplify equation (6) by linearizing it assuming small perturbations in both Δ and the phase space trajectories. From the metric, using the fact that we defined n^i to be the photon direction measured by a fundamental observer in an orthonormal frame, we have

$$\frac{(1-\psi)}{(1+\phi)}\frac{dx^i}{d\tau} = n^i . \tag{7}$$

Thus, treating both the metric perturbations and Δ as being of the same order, we can replace $dx^i/d\tau$ by n^i in equation (6). A similar argument shows that we can drop the $(\partial\Delta/\partial n^i)(dn^i/d\tau)$ term: both factors are first-order quantities. This is equivalent to neglecting gravitational lensing of anisotropies. Lensing by nonlinear (highly overdense) structures at low redshift has a small effect on the CMB on arcminute angular scales (Seljak 1996).

We are left with calculating the rate of change of proper energy E, which is straightforward from the geodesic equation. The result is

$$\frac{d\ln(aE)}{d\tau} = -n^i\partial_i\phi + \partial_\tau\psi \ . \tag{8}$$

The factor a accounts for the cosmological redshift while the first term on the right-hand side is the familiar gravitational redshift. (Both terms arise from g_{00}.) The second term, due to spatial curvature fluctuations, is unfamiliar in the Newtonian limit but can be significant for photons and other relativistic particles.

Because the right-hand side of equation (8) is independent of E, it follows that the $d\ln(aE)/d\tau$ contribution to equation (6) cannot induce any energy-dependence of the brightness temperature perturbation. (As in gravitational lensing, gravity is "achromatic.") The dominant collision process, Compton scattering, is also independent of energy (at temperatures much less than the electron mass). Thus, unless some other physical process causes a departure of the photon spectrum from blackbody, $\partial\Delta/\partial E = 0$ to an excellent approximation. None of the standard sources of primary anisotropy (primeval potential, density, or entropy perturbations) generates any significant blackbody distortion, so we assume $\partial\Delta E = 0$ in the following. (Departures of order the baryon-to-photon ratio 10^{-10} are generated during recombination, but these are orders of magnitude smaller than the effects we retain.)

Combining equations (6), (7), and (8), we obtain the fundamental equation of CMB anisotropy:

$$\frac{d\Delta}{d\tau} = \partial_\tau\Delta + n^i\partial_i\Delta = -n^i\partial_i\phi + \partial_\tau\psi + \left(\frac{d\Delta}{d\tau}\right)_c \ . \tag{9}$$

Equation (9) has a very simple physical interpretation. Aside from changes due to gravitational redshift, time-varying spatial curvature fluctuations, or radiative processes (emission, absorption, and scattering), the CMB anisotropy (brightness temperature fluctuation) is constant along null geodesics.

For completeness, we present without derivation the collision terms arising from nonrelativistic photon-electron scattering:

$$\left(\frac{d\Delta}{d\tau}\right)_{\rm c} = an_e\sigma_{\rm T}\left(-\Delta + \frac{1}{3}\delta_\gamma + v_e^i n_i + \frac{1}{2}\Pi^{ij}n_i n_j\right) \tag{10}$$

where $\sigma_{\rm T}$ is the Thomson cross section and the factor outside the parentheses on the right-hand side is the Thomson scattering rate (up to a factor $c = 1$). The electrons have proper number density n_e and peculiar velocity v_e^i. (The unperturbed electron density may be used when considering primary anisotropies because the terms in parentheses are all first-order perturbations.) The photon number density fluctuation is $\delta_\gamma \equiv \delta n_\gamma/\bar{n}_\gamma = \frac{3}{4}\delta\rho_\gamma/\bar{\rho}_\gamma$ where n_γ and ρ_γ are the photon number density and energy density, respectively. The perturbation can be obtained from an angular average of the anisotropy: $\delta_\gamma = 3\int \Delta\, d\Omega/(4\pi)$. (Note that $n_\gamma \propto T^3$ implies $\delta_\gamma = 3\delta \ln T$.)

Heuristically, equation (10) is easy to understand. Scattering corresponds to absorption (the $-\Delta$ term) and re-radiation in a different direction. To the extent that the scattering is isotropic in the electron frame, the emitted radiation is just the angular average of the absorbed radiation ($\frac{1}{3}\delta_\gamma$ is the angular average of Δ). Scattering therefore isotropizes the radiation field, a phenomenon familiar to anyone driving a car through fog. The second term is due to the motion of the electron gas: scattering by moving targets introduces a dipole anisotropy.

The third term, $\Pi^{ij}n_i n_j$, arises from the dependence of Thomson scattering on direction and polarization. It is easy to understand qualitatively from Rayleigh's Law of scattered light. When a photon scatters from an electron, the incoming and outgoing momenta lie in a plane called the scattering plane. The photon is polarized with its electric field orientation either in the plane or perpendicular to it. In the former case, the scattered flux is reduced by a factor $\cos^2\theta$ compared with the perpendicular case where θ is the scattering angle. This result follows classically from the angular dependence of electric dipole radiation caused when the incoming light makes the electron oscillate. Another way to express the same result is to say that the scattering rate is proportional to $(\vec{\epsilon}_1 \cdot \vec{\epsilon}_2)^2$ where $\vec{\epsilon}_1$ and $\vec{\epsilon}_2$ are the polarization directions for the incoming and outgoing photons, respectively.

These considerations imply that the differential cross section for unpolarized incident radiation is proportional to $1 + \cos^2\theta$. Normalizing the total cross section, we find

$$\frac{d\sigma}{d\Omega} = \frac{3\sigma_{\rm T}}{16\pi}(1 + \cos^2\theta)\ . \tag{11}$$

If the incident radiation is polarized, then the cross-section becomes a 2×2 matrix giving scattering rates for each orthogonal polarization. Thus, the dependence of the scattering rate on polarization and direction add corrections to the isotropic scattering implied by the $-\Delta + \frac{1}{3}\delta_\gamma$ terms in equation (10). These corrections are only a few percent for the temperature anisotropy but they are crucial for polarization. Scattering induces a small polarization of the CMB. We will ignore the polarization and the quadrupolar scattering term $\Pi^{ij}n_i n_j$ in the following.

Note that the unperturbed (spatially homogeneous) electron density may be used in equation (10) because it multiplies a first-order quantity. Spatial variations in the

electron density only appear in second-order perturbation theory.

In evaluating the primary CMB anisotropy, we need not take into account that recombination takes place at different times in different places. The reason physically is that the radiation field is in nearly perfect thermal equilibrium with the electrons. For perfect (everywhere homogeneous and isotropic) blackbody radiation, nonrelativistic scattering by an electron gas at rest with respect to the radiation field has no effect whatsoever on the radiation. In the absence of pre-existing CMB fluctuations, scattering alone cannot produce any anisotropy no matter how inhomogeneous the electron distribution. The only possible effect occurs from the motion of the electron gas, and this is included already in equation (10).

3.2 Solution of the radiative transfer equation

We can easily integrate equation (9) in the instantaneous recombination approximation, in which we assume that n_e drops sharply to zero at $\tau = \tau_{\rm e}$. Prior to this time the photon mean-free path is very short; we assume it is effectively zero. Under these conditions, integrating equation (9) along the backwards light cone to $\chi_{\rm e} \equiv \tau_0 - \tau_{\rm e}$ gives the desired CMB anisotropy seen by the fundamental observer at $\chi = 0$:

$$\Delta_0(n^i) = \Delta_{\rm e} + \phi_{\rm e} - \phi_0 + \int_0^{\chi_{\rm e}} d\chi\, \partial_\tau(\phi + \psi)_{\rm ret} \tag{12}$$

where subscript "e" means to evaluate the quantity at $\tau = \tau_{\rm e}$, $\chi = \chi_{\rm e} = \tau_0 - \tau_{\rm e}$, in direction $-n^i$ (with a minus sign because the photon travels toward decreasing χ). Subscript "ret" means to evaluate the quantity in the integrand at retarded time $\tau = \tau_0 - \chi$.

The first three terms on the right-hand side of equation (12) are all boundary terms which arise as constants of integration. The first two represent brightness temperature and gravitational potential fluctuations present at recombination and are the major contributors to CMB anisotropy. The third term, the gravitational potential at $\chi = 0$, is an unobservable monopole contribution. The integral term is anisotropy produced *after* recombination due to time-changing gravitational potentials.

Before examining the physical content of equation (12) in the next section, it is instructive to compare with the exact solution of the full radiative transfer equation. Including the Thomson scattering terms of equation (10), equation (9) has solution (Seljak & Zaldarriaga 1996)

$$\Delta_0(n^i) = \int_0^{\tau_0} d\chi\, e^{-\tau_{\rm T}(\chi)} \left[-n^i \partial_i \phi + \partial_\tau \psi + a n_e \sigma_{\rm T} \left(\frac{1}{3}\delta_\gamma + v_e^i n_i + \frac{1}{2}\Pi^{ij} n_i n_j \right) \right]_{\rm ret} \tag{13}$$

where

$$\tau_{\rm T}(\chi) \equiv \int_0^{\chi} d\chi\, (a n_e \sigma_{\rm T})_{\rm ret} \tag{14}$$

is the Thomson optical depth (and *not* a conformal time). Equation (13) is the familiar solution of the radiative transfer equation. Emission (the terms in square brackets) at optical depth $\tau_{\rm T}$ is reduced by an exponential absorption factor. In contrast with equation (12), there is no explicit indication of the photosphere. The radial integration is taken over the entire past lightcone to $\tau = 0$ ($\chi = \tau_0$). Contributions from $\chi > \chi_{\rm e}$ (which may be defined by $\tau_{\rm T}(\chi_{\rm e}) = \frac{1}{3}$ as in stellar astrophysics) are exponentially suppressed.

Equation (13) may be clarified by defining the integral visibility function

$$\zeta(\tau) \equiv \exp\left[-\int_\tau^{\tau_0} d\tau'\, a(\tau') n_e(\tau') \sigma_{\rm T}\right] = \exp\left[-\tau_{\rm T}(\tau_0 - \tau)\right] \ . \tag{15}$$

This function rises rapidly from zero to unity as τ increases through $\tau_{\rm e}$. The conformal time derivative $d\zeta/d\tau = a n_e \sigma_{\rm T} \exp(-\tau_{\rm T})$ is precisely the factor multiplying the scattering terms in equation (13).

The spatial derivative term in equation (13) may be converted into a convective derivative through $-n^i \partial_i = -(d/d\tau) + \partial_\tau$. The convective derivative term (but not the partial derivative terms) may be integrated by parts. Using the function $\zeta(\tau)$ defined above, we obtain

$$\begin{aligned} \Delta_0(n^i) = \quad & \int_0^{\tau_0} d\chi\, \dot\zeta(\tau_0 - \chi) \left(\phi + \frac{1}{3}\delta_\gamma + v_e^i n_i + \frac{1}{2}\Pi^{ij} n_i n_j\right)_{\rm ret} \\ & + \int_0^{\tau_0} d\chi\, \zeta(\tau_0 - \chi) \partial_\tau \left(\phi + \psi\right)_{\rm ret} \end{aligned} \tag{16}$$

where we have discarded the unobservable monopole $-\phi_0$.

Equation (16) simplifies in the instantaneous recombination approximation, for which $\zeta(\tau)$ is a unit step function at $\tau = \tau_{\rm e}$ and $\dot\zeta = \delta_{\rm D}(\tau - \tau_{\rm e})$ is a Dirac delta function. In this limit, we recover equation (12) with

$$\Delta_{\rm e} = \left(\frac{1}{3}\delta_\gamma + v_e^i n_i + \frac{1}{2}\Pi^{ij} n_i n_j\right)_{\rm e} \ . \tag{17}$$

Equation (16) also shows us the effects of a finite width to the cosmic photosphere. The primary contributions multiplying $\dot\zeta$ are averaged over the finite timespan of recombination while the effects of the time derivatives of the potentials turn on gradually during recombination. (As a result, the time derivative terms make a significant contribution to anisotropy in models with low Ωh^2, because then recombination occurs only a little after the universe becomes matter-dominated, while the potentials are still changing.)

4 Contributions to Primary Anisotropy

In the instantaneous recombination approximation, there are a total of four contributions to primary CMB anisotropy measured by a fundamental observer: intrinsic, Doppler,

gravitational, and integrated Sachs-Wolfe. We will discuss them in turn so as to give a physical interpretation to the sources of CMB anisotropy.

The intrinsic and Doppler anisotropies correspond to the first term in equation (12), i.e. the brightness temperature perturbation $\Delta_{\rm e}$ present at the time of recombination. Equation (17) gives this term. However, further simplification results because of the tight coupling of photons and baryons (and electrons) prior to recombination. Under these conditions, $v_e^i = v_\gamma^i$. Also, the intrinsic quadrupole anisotropy source term due to polarization effects vanishes because multiple scattering prior to recombination damps the polarization caused by single scattering. This is the reason why CMB polarization is predicted to be so small (Zaldarriaga & Seljak 1997; Spergel & Zaldarriaga 1997).

Thus, in the instantaneous recombination approximation, we may write

$$\Delta_{\rm e} \approx \left(\frac{1}{3}\delta_\gamma + n_i v_\gamma^i\right)_{\rm e} \ . \tag{18}$$

This gives the explicit form of the intrinsic ($\frac{1}{3}\delta_\gamma$) and Doppler ($n_i v_\gamma^i$) contributions. (Recall that $\delta_\gamma = \frac{3}{4}\delta\rho_\gamma/\bar{\rho}_\gamma$.) It has a simple interpretation which does not require the full treatment of scattering used in deriving equation (16). In the instantaneous recombination approximation, the photon-baryon gas is a perfect fluid up to the moment of recombination. In the rest frame of this fluid, the radiation is isotropic blackbody radiation at temperature T. Spatial variations of T translate into number density variations $\delta_\gamma = 3\delta\ln T$, explaining the first term. But the photon-baryon fluid moves with a local three-velocity v_γ^i. (Fluids flow!) For small velocities, the linear Doppler formula gives a brightness temperature shift $n_i v_\gamma^i$. In some directions, the photosphere is moving toward us (relative to unperturbed Hubble expansion) while in other places it recedes, producing anisotropy in the emitted radiation.

The next contribution to anisotropy in equation (12) is the gravitational redshift $\phi_{\rm e} - \phi_0$. Each photon travelling to us falls through a gravitational potential difference $\phi_{\rm e} - \phi_0$ and the energies are changed correspondingly.

The literature contains some misstatements about the gravitational redshift effect. The primary anisotropy for isentropic fluctuations on large scales is $\Delta = \frac{1}{3}\phi_{\rm e}$ (Sachs & Wolfe 1967), a factor of 3 different from the gravitational redshift anisotropy to which it is sometimes erroneously ascribed. We will see below that the Sachs-Wolfe result comes from combining the intrinsic anisotropy ($\frac{1}{3}\delta_\gamma$) and gravitational redshift effects. (Moreover, it is valid only for isentropic fluctuations but not for isocurvature ones. More on that below.)

The final contribution to anisotropy comes from the integral term in equations (12) and (16), which is commonly called the "Integrated Sachs-Wolfe" term. If the gravitational potential changes with time, photons suffer different amounts of gravitational redshift falling into and climbing out of potential wells between recombination and today. (This effect on the CMB was first pointed out by Rees & Sciama in 1968.) However, a

Newtonian-inspired calculation (Rees & Sciama 1968) would include only the $\partial_\tau\phi$ term because $\partial_\tau\psi$ is due to space curvature and has no effect on nonrelativistic particles (nor does it have any Newtonian interpretation). But just as the deflection of light in a weak gravitational field is twice the Newtonian-inspired value, if $\psi = \phi$ the change in energy due to a time-varying potential is twice the result from $\partial_\tau\phi$.

Note that the integrated Sachs-Wolfe term is the only contribution to anisotropy in the linear regime (i.e. arising from linearized fluctuations) that is produced *after* recombination. In most models the contribution is small, although there is a measurable effect on large angular scale anisotropy in models with curvature and/or vacuum energy.

5 Evolution of Matter and Metric Perturbations

To evaluate the solutions given above (e.g. eqs. 12 plus 18 in the instantaneous recombination approximation) we must determine the density, velocity, and gravitational potential fluctuations present at the time of recombination (and later, to get the integrated Sachs-Wolfe contribution). This is non-trivial. Accurate results can be obtained only by integrating numerically two of equations (19)–(23) plus the coupled relativistic perturbation equations for photons, baryons, neutrinos, dark matter, and any other components present in the universe (e.g. Ma & Bertschinger 1995; Seljak & Zaldarriaga 1996). This integration is performed numerically by the CMBFAST code of Seljak & Zaldarriaga as well as by its slower predecessors (e.g. Ma & Bertschinger 1995).

Despite the complexity of this evolution, we can learn a great deal by examining the behavior on large scales and at early times in the universe. In this section we will derive the equations of motion for the metric and the coupled fluids responsible for metric perturbations. We will solve these analytically on large scales. This approach gives good physical insight to the various sources of CMB anisotropy.

5.1 Einstein equations

The Einstein equations for metric (1) are given by Bertschinger (1996); beware that ϕ and ψ are reversed there.

The 00 Einstein equation give

$$\left(\nabla^2 + 3K\right)\psi - 3\frac{\dot{a}}{a}\left(\partial_\tau\psi + \frac{\dot{a}}{a}\phi\right) = 4\pi G a^2 \delta\rho \tag{19}$$

where $\delta\rho = \rho - \bar{\rho}(t)$ is the perturbation in the proper energy density at (x^i, τ) measured by a fundamental observer and K is the spatial curvature constant of a non-flat Robertson-Walker background spacetime. (We reserve the lower-case k for comoving wavenumber below.) Although we will later drop curvature, it is included here for completeness.

The $0i$ component of the Einstein equations helps us to understand the time-derivative terms in equation (19):

$$\nabla^2 \left(\partial_\tau \psi + \frac{\dot{a}}{a} \phi \right) = -4\pi G a^2 \nabla_i \left[(\rho + p) v^i \right] \ . \tag{20}$$

The term in brackets is the momentum density measured by a fundamental observer, or T^{0i} in an orthonormal basis. In general relativity, momentum density (and momentum flux, i.e. stress) is a source of spacetime curvature. The momentum density, hence its effect on curvature, is typically smaller than $\delta\rho$ by a factor v/c. However, it is gravitationally significant on large scales (Hubble-length and beyond). Thus, the time-derivative terms in equation (19) are unimportant on scales much less than the Hubble length but are important on larger scales. They are important for CMB anisotropy on scales larger than a degree or so.

With the neglect of gravitomagnetism and gravitational radiation, the metric perturbations follow from spatial scalars and not, for example, a vector potential (Bertschinger 1996). In the limit of small fluctuations, it follows that the velocity fields of the various matter and radiation components are the gradients of scalar fields. That is, the velocity fields have no vorticity (or are longitudinal, in the language of classical field theory). Using this fact, we may write

$$v_a^i = -\gamma^{ij} \nabla_j u_a \tag{21}$$

for the mean (fluid) velocity of any component a (e.g. photons, baryons, CDM, neutrinos) where $u(x^i, \tau)$ is the velocity potential and γ^{ij} is the inverse of the unperturbed spatial 3-metric γ_{ij} defined so that the comoving spatial line element is $dl^2 = \gamma_{ij} dx^i dx^j$ in equation (1). This fact allows us to combine equations (19) and (20) into a cosmological Poisson equation,

$$\left(\nabla^2 + 3K \right) \phi = 4\pi G a^2 \sum_a \left[\delta\rho_a + 3 \frac{\dot{a}}{a} (\rho_a + p_a) u_a \right] \ . \tag{22}$$

Aside from the curvature and velocity potential terms, equation (22) is an obvious generalization of the Newtonian Poisson equation. The source for the metric perturbation must be $\delta\rho$ rather than ρ because $\phi = \psi = 0$ for an unperturbed Robertson-Walker spacetime with $\rho = \bar{\rho}$. The presence of the velocity potential shows that, in cosmology, momentum as well as mass-energy is a source for Newtonian gravity. This should not be surprising, given that momentum in one Lorentz frame transforms into energy in another frame. It can be shown that a small, spatially-varying transformation of the time coordinate can be performed which eliminates the momentum density (basically by transforming to the local fluid rest frame) and thereby converts the term in brackets to a pure density fluctuation (Bardeen 1980). However, it proves more convenient to use the coordinates implied by equation (1) and simply evaluate both the density and momentum contributions to gravity in these coordinates. (For a discussion of other coordinate systems, see Bardeen 1980 and Bertschinger 1996.)

The summed ii components of the Einstein equations give a result that will be useful later:

$$\partial_\tau^2\psi - K\psi + \frac{\dot{a}}{a}\,\partial_\tau(\phi + 2\psi) + \left[2\frac{d}{d\tau}\left(\frac{\dot{a}}{a}\right) + \left(\frac{\dot{a}}{a}\right)^2\right]\phi + \frac{1}{3}\nabla^2(\phi - \psi) = 4\pi G a^2 \delta p \qquad (23)$$

where $\delta p = p - \bar{p}$ is the perturbation in the pressure (isotropic stress).

Finally, the trace-free part of the ij components of the Einstein equations give a relation between the two gravitational potentials:

$$\left(\nabla_i\nabla_j - \frac{1}{3}\gamma_{ij}\nabla^2\right)(\psi - \phi) = 8\pi G a^2 \Sigma_{ij,\perp} \qquad (24)$$

where $\Sigma_{ij,\perp}$ is the longitudinal shear stress. Longitudinal shear stress arises from quadrupole anisotropy in the angular distribution of the particle momenta; for a weakly imperfect fluid it is the stress arising from shear viscosity. A perfect fluid has no shear stress. The major contribution to $\Sigma_{\rm ij,\perp}$ comes from massless neutrinos; photons make a small contribution after recombination. When the universe becomes matter-dominated, $\Sigma_{\rm ij} \ll \delta\rho$ and therefore $|\psi - \phi|$ is small compared with ϕ. In the following we will neglect shear stress, with resulting errors of order one percent in the CMB anisotropy. For a full treatment including shear stress, see Ma & Bertschinger (1995).

5.2 Fluid equations

The Einstein equations (19)–(23) require that we specify the density, velocity, and pressure perturbations of matter and radiation. We will approximate the contents of the universe before recombination by two decoupled perfect fluids: cold dark matter and the photon-baryon plasma. Cold dark matter is a pressureless fluid that interacts only by gravity. Photons are tightly coupled to electrons by Thomson scattering, which are themselves tightly coupled to protons and helium atoms and ions by Coulomb scattering. We apply this description at temperatures below 1 MeV, after electron-positron annihilation and neutrino decoupling. Thus the neutrinos should be regarded as a third, decoupled gas. Their finite temperature and lack of collisions make the neutrinos an imperfect gas. We will discuss the neutrinos below.

The fluid equations follow from $\nabla_\mu T^{\mu\nu} = 0$ applied to a perfect fluid with stress-energy tensor $T^{\mu\nu} = (\rho + p)V^\mu V^\nu + p g^{\mu\nu}$ where V^μ is the 4-velocity. We define the three-velocity $v^i = V^i/V^0$. Working to first order in the metric perturbations and the fluid 3-velocity, we find

$$\begin{aligned}
&\partial_\tau\rho + 3\left(\frac{\dot{a}}{a} - \partial_\tau\psi\right)(\rho + p) + \nabla_i\left[(\rho + p)v^i\right] = 0\ , \\
&\partial_\tau\left[(\rho + p)v^i\right] + 4\frac{\dot{a}}{a}(\rho + p)v^i + \nabla_i p + (\rho + p)\nabla_i\phi = 0\ .
\end{aligned} \qquad (25)$$

It is easy to interpret the various terms in equations (25). The terms proportional to $\dot{a}/a$ are "Hubble damping" terms arising because we are using comoving coordinates. The $\partial_\tau \psi$ term appears in the continuity equation because, from the metric (1), the homogeneous expansion factor $a(\tau)$ is effectively modified by spatial curvature perturbations to become $a(1-\psi)$. The pressure p is present with ρ in the energy flux (momentum density) because we let ρ be the energy density (not the rest-mass density), which is affected by the work done by pressure forces in compressing the gas.

For convenience in what follows, we define the perturbation in energy density relative to the enthalpy density $\rho + p$,

$$\delta \equiv \frac{\delta\rho}{\bar{\rho} + \bar{p}} \ . \tag{26}$$

Beware, this is a non-standard notation: most authors (including the present one in the papers listed in the bibliography) define $\delta \equiv \delta\rho/\bar{\rho}$. For cold dark matter, with $\bar{p} = 0$, there is no difference. However, for photons or other relativistic particles, $\bar{p}/\bar{\rho}$ is nonzero. Our definition of δ agrees with Weinberg (2002). It has a simple physical interpretation: δ is the fractional perturbation in the number density or particles (rather than the energy density of particles). This choice simplifies the equations and calculations that follow.

The unperturbed matter and radiation fluids are perfect fluids, i.e. they have zero shear stress. For these fluids, $w = p/\rho$ depends only on ρ. The speed of sound for a fluid component is $c_{\rm s} = (dp/d\rho)^{1/2}$. Linearizing equations (25) about the unperturbed solution and using equation (26), we now obtain (cf. Ma & Bertschinger 1995)

$$\begin{aligned} \partial_\tau \delta &= (\nabla^2 u + 3\partial_\tau \psi) \ , \\ \partial_\tau u + \frac{\dot{a}}{a}(1 - 3c_{\rm s}^2)u &= c_{\rm s}^2 \delta + \phi \ . \end{aligned} \tag{27}$$

We have used the assumption of potential flow, equation (21).

Our goal now is to obtain equations of motion for the density and velocity potentials of our two fluids, CDM and the photon-baryon plasma. The CDM case is simple with $w = c_{\rm s}^2 = 0$. The photon-baryon plasma is more complicated. First let us consider the perturbations of photons and baryons separately. Because of the large photon-to-baryon ratio (about 2×10^9), a negligible amount of heat is transferred to photons from baryons compared with the energy in the photons. Thus, photons with density perturbation δ_γ obey the first of equations (27) with $w = \frac{1}{3}$ while baryons with density perturbation δ_b obey the same equation with $w = 0$ (since they are nonrelativistic). Now, the tight coupling due to Thomson scattering ensures that the photons and baryons have a common velocity potential, $u_b = u_\gamma$. Thus, if the photon-to-baryon ratio was unperturbed initially, it follows from the first of equations (27) that $\delta_b = \delta_\gamma$. With equation of state $w = \bar{p}/\bar{\rho} = \bar{p}_\gamma/(\bar{\rho}_\gamma + \bar{\rho}_b)$, we get

$$c_{\rm s}^2 = \frac{d\bar{p}_\gamma/d\tau}{d(\bar{\rho}_b + \bar{\rho}_\gamma)/d\tau} = \frac{1}{3}\left(1 + \frac{3}{4}y_b\right)^{-1} \quad , \quad y_b \equiv \frac{\bar{\rho}_b}{\bar{\rho}_\gamma} \ . \tag{28}$$

Combining all our results, the perturbed fluid equations for CDM (subscript c) and the photon-baryon fluid (subscript γ) are

$$\begin{aligned}
\partial_\tau \delta_c &= \nabla^2 u_c + 3\partial_\tau \psi \ , \\
\partial_\tau u_c &= -\frac{\dot{a}}{a} u_c + \phi \ , \\
\partial_\tau \delta_\gamma &= \nabla^2 u_\gamma + 3\partial_\tau \psi \ , \\
\partial_\tau u_\gamma &= c_{\rm s}^2 \left(\delta_\gamma - \frac{9 y_b}{4} \frac{\dot{a}}{a} u_\gamma \right) + \phi \ .
\end{aligned} \tag{29}$$

These agree with equations (3) of Seljak (1994) if neutrino shear stress is neglected so that $\psi = \phi$. They are valid on all length scales provided that the photons are tightly coupled to the baryons.

Equations (29) must be supplemented by an equation for the gravitational potential ϕ. We have a choice of equations (19)–(23). If we evolve the matter and radiation exactly, then all of these components of the Einstein equations are equivalent. We will choose a linear combination involving the effective sound speed squared

$$c_w^2 \equiv \frac{d\bar{p}/d\tau}{d\bar{\rho}/d\tau} = \frac{1}{3} \left(1 + \frac{3}{4} y \right)^{-1} \quad , \quad y \equiv \frac{\bar{\rho}_b + \bar{\rho}_c}{\bar{\rho}_\gamma + \bar{\rho}_\nu} \ . \tag{30}$$

Note that c_w would be the speed of sound if all matter (CDM and baryons) were tightly coupled to all radiation (photons and neutrinos). However, because this multi-component medium is not a single perfect fluid, c_w is not a true sound speed. Nonetheless, it is a useful quantity for obtaining a physical evolution equation for the gravitational potential.

We choose a linear combination of equations (19)–(23) that yields the simplest description of motion, by multiplying equation (19) by c_w^2 and subtracting it from equation (23). Using equation (2), and setting $\psi = \phi$, the resulting perturbed Einstein equation is (Bardeen 1980)

$$\begin{aligned}
\partial_\tau^2 \phi + 3(1 + c_w^2) \frac{\dot{a}}{a} \partial_\tau \phi &+ \left[3(c_w^2 - w) \left(\frac{\dot{a}}{a} \right)^2 - (5 + 3w) K \right] \phi - c_w^2 \nabla^2 \phi \\
&= 4\pi G a^2 (\delta p - c_w^2 \delta \rho) \equiv \frac{c_w^2}{y} \nabla^2 \sigma \ ,
\end{aligned} \tag{31}$$

where σ is a dimensionless entropy potential that will be discussed below, and

$$w \equiv \frac{\bar{p}}{\bar{\rho}} = \frac{1}{3(1+y)} \ . \tag{32}$$

In equation (31), δp and $\delta \rho$ are the total pressure and energy density perturbations summed over baryons, cold dark matter, photons, and neutrinos. Let us approximate

the behavior of the neutrinos by supposing that they trace photons, with $\delta_\nu = \delta_\gamma$ and $\delta p_\nu/\bar{\rho}_\nu = \delta p_\gamma/\bar{\rho}_\gamma$. This is not correct on scales smaller than the Hubble length, but it is a good approximation on larger scales because the neutrinos have then not yet had enough time to separate from the photons. Our assumption overestimates the neutrino perturbations on small scales because, in the absence of collisions, neutrinos easily diffuse out of perturbations. However, the effects of this error are not large because the gravitational effect of neutrinos is important only during the radiation-dominated era, and during this time the photon perturbations rapidly oscillate on small scales so that their time average is small. Doing better would require that we solve the Boltzmann equation for neutrinos (Ma & Bertschinger 1995), which will not be discussed here.

The source term in equation (31) is proportional to the entropy per unit mass of cold dark matter,

$$\delta\left(\ln\frac{T_\gamma^3}{\rho_c}\right) = \delta_\gamma - \delta_c = \frac{\delta p - c_w^2\delta\rho}{\bar{\rho}_c c_w^2} \ , \tag{33}$$

so that

$$\nabla^2\sigma = 4\pi G a^2 \bar{\rho}_c y \left(\delta_\gamma - \delta_c\right) \ . \tag{34}$$

Neutrino effects are included implicitly through the effective sound speed c_w.

Equation (31) is rather remarkable. It allows us to compute the gravitational potential through a damped, driven *wave equation* whose source is the specific entropy perturbation. In Newtonian gravitation we think of the potential as being determined by action-at-a-distance (eq. 19 without the time-derivative terms). However, the Einstein equations also enforce local energy-momentum conservation, providing us with alternatives for the computation of the metric perturbations. Heuristically, the potential ϕ is computed from the instantaneous distribution of energy density (and momentum density, as may be shown by combining eqs. 19 and 20). Because the source of the potential may have acoustic waves, then it, too, displays acoustic waves. Note that the wave speed is the effective sound speed c_w.

True gravitational waves (which propagate at c) are described by a transverse-traceless metric perturbation h_{ij}, which we are ignoring here. Thus, despite its appearance, equation (31) really is gravitational action-at-a-distance. Although gravitational waves are needed to restore causality, we are ignoring them here for the CMB anisotropy calculation. This is justified in linear perturbation theory by the fact that gravity waves have no coupling to the "scalar-mode" (density and entropy) perturbations we are considering here. In linear perturbation theory, the effects of density and entropy perturbations propagate at the speed of sound, not the speed of light.

Our next step is to obtain an evolution equation for the entropy potential σ. Using the fact that $a^2\bar{\rho}_c y$ is constant, from equations (34) together with equations (28)–(30) we obtain

$$\partial_\tau^2\sigma + \left(1 + 3c_w^2 - 3c_{\rm s}^2\right)\frac{\dot a}{a}\,\partial_\tau\sigma - (c_{\rm s}^2 - c_w^2)\nabla^2\sigma$$
$$= 4\pi G a^2 y(c_{\rm s}^2 - c_w^2)\left[\bar\rho_c\left(\delta_c + 3\frac{\dot a}{a}u_c\right) + \frac{3}{4}\frac{c_w^2}{c_{\rm s}^2 - c_w^2}\,\bar\rho_c\left(\delta_\gamma + 4\frac{\dot a}{a}u_\gamma\right)\right] . \qquad (35)$$

Using equations (28) and (30), we obtain

$$\frac{3}{4}\frac{c_w^2}{c_{\rm s}^2 - c_w^2}\,\bar\rho_c = \left[\bar\rho_\gamma + \bar\rho_\nu + \frac{3}{4}\bar\rho_b\left(1 + \frac{\bar\rho_\nu}{\bar\rho_\gamma}\right)\right]\left(1 - \frac{\bar\rho_b\bar\rho_\nu}{\bar\rho_c\bar\rho_\gamma}\right)^{-1} . \qquad (36)$$

Using this result, if we compare the right-hand sides of equations (22) and (35), we see that they would be identical for our multicomponent fluid if we neglect neutrinos. Including neutrinos requires approximation because we are not solving the Boltzmann equation for neutrinos. One approximation is to suppose that neutrinos have identical density and velocity perturbations as photons. Under this assumption, ρ_γ would simply be replaced by $\rho_\gamma + \rho_\nu$ in equation (22) and similarly for p_γ. This assumption was made in deriving equations (33) and (35). However, we know that this approximation is not exact, and so we are free to consider other approximations that make errors of the same order. That is, we can consider corrections to equation (36) that are of order $\bar\rho_\nu$.

We choose to approximate the right-hand side of equation (36) by dropping the factors in parentheses (Bashinsky & Bertschinger 2002). This approximation is exact when neutrinos are neglected. The reason for making this choice is that now equations (35) becomes a simple wave equation that is very similar to equation (31),

$$\partial_\tau^2\sigma + \left(1 + 3c_w^2 - 3c_{\rm s}^2\right)\frac{\dot a}{a}\,\partial_\tau\sigma - (c_{\rm s}^2 - c_w^2)\nabla^2\sigma = y(c_{\rm s}^2 - c_w^2)\left(\nabla^2 + 3K\right)\phi . \qquad (37)$$

This equation is exact only when neutrinos are neglected. However, as we will see in Section 7, when neutrinos are included it preserves the correct propagation of sound waves through the photon-baryon fluid at sound speed $c_{\rm s}$.

The two-fluid approximation introduced here is equivalent to including neutrinos assuming that they have the same dynamics as photons. The baryon abundance is increased over the true abundance by a factor $(1 + \bar\rho_\nu/\bar\rho_\gamma)$ so that the photon-baryon sound speed is unchanged. Finally, the CDM abundance is decreased so that the total matter density $\bar\rho_c + \bar\rho_b$ is unchanged. This model has the advantage of preserving the important time and length scales $\tau_{\rm eq}$ and $\int c_{\rm s}\,d\tau$ while working with perfect fluids. For more discussion of the two-fluid approximations, see Bashinsky & Bertschinger (2002).

Equations (31) and (37) completely characterize the evolution of matter, radiation, and gravity in our simplified two-fluid model (CDM and the photon-baryon fluid, with neutrinos added in a way that preserves the photon-baryon sound speed). Because

of the modification made in deriving equation (37), these equations are not exactly equivalent to the fluid equations (29) plus the Poisson equation (22) when neutrinos are included. They agree with the approximations made by Seljak (1994) and Bashinsky & Bertschinger (2001, 2002). We will find in Section 9 that the two-fluid approximation made here is remarkably accurate.

6 Large-scale anisotropy: the Sachs-Wolfe Effect

Using the wave equations we have derived for the gravitational potential ϕ and entropy potential σ, it is possible analytically to solve for the perturbations on large scales. In this context, "large scale" means that we can neglect $c_w^2\nabla^2$ and $c_{\rm s}^2\nabla^2$ relative to $(\dot{a}/a)^2$ in equations (31) and (37). This is valid provided that we consider scales larger than the comoving *acoustic length*, defined by

$$L_{\rm ac} \equiv \frac{c_{\rm s}}{aH} \ . \tag{38}$$

The acoustic length subtends an angle of about one degree at recombination. We also will neglect the spatial curvature K, which makes a negligible contribution to equations (31) and (37) before and during recombination because $|K| \ll (\dot{a}/a)^2$.

Under these conditions, equations (31) and (37) reduce to ordinary differential equations in time. We change variables from τ to y through equation (3), obtaining

$$y\phi'' + \frac{y\phi'}{2(1+y)} + 3\left(1+c_w^2\right)\phi' + \frac{3c_w^2\phi}{4(1+y)} = \frac{(c_w\tau_e)^2}{(1+y)}\,\nabla^2\sigma \tag{39}$$

and

$$y\sigma'' + \frac{y\sigma'}{2(1+y)} + \left(1+3c_w^2-3c_{\rm s}^2\right)\sigma' = \frac{(c_{\rm s}^2-c_{\rm y}^2)\tau_e^2}{1+y}\,y^2\nabla^2\phi \ , \tag{40}$$

where a prime denotes ∂_y. We have retained the Laplacian terms that link the potential and density because we have said nothing yet about the relative sizes of ϕ and σ.

As $y \to 0$, the gravitational potential makes a negligible contribution to σ in equation (40), at least insofar as that contribution feeds back to equation (39). Thus, in solving for the gravitational potential it is safe to drop the right-hand side of equation (40), which then becomes an ordinary differential equation in y whose solutions as $y \to 0$ are $\sigma \propto \ln y$ and $\sigma = \sigma(x)$ with $\partial_y\sigma = 0$. The logarithmic solution is unphysical; it corresponds to a large separation between photons and CDM at the big bang, which does not occur in standard cosmology. Thus, the only possibility for the entropy is to have a constant or spatially-varying distribution of primeval entropy fluctuations that is constant in time early in the radiation era.

Given the time-independent solution for the entropy σ, it is easy to solve equation (39) for $\phi(y)$. The homogeneous ($\sigma = 0$) solutions for $\phi(y)$ are (Kodama & Sasaki 1984, 1986)

$$\phi_1(y) = 1 + \frac{2}{9y} - \frac{8}{9y^2} - \frac{16}{9y^3} + \frac{16}{9}\frac{\sqrt{1+y}}{y^3} \ , \quad \phi_2(y) = \frac{\sqrt{1+y}}{y^3} \ . \tag{41}$$

For $y \ll 1$, $\phi_1 = \frac{10}{9}(1 - \frac{1}{16}y + \cdots)$. The density perturbations associated with ϕ_1 grow in the matter-dominated era $y \gg 1$ (hence ϕ_1 is often called the growing mode) although ϕ_1 itself does not. The other mode, ϕ_2, is called the decaying mode. From the these homogeneous solutions, we can construct particular solutions subject to any desired initial conditions. Using the Green's function method we can also construct solutions with nonzero $\nabla^2\sigma$.

Before presenting the solutions, we recall from equation (13) that the CMB anisotropy computation requires δ_γ and v^i_γ in addition to ϕ. On large scales, where pressure-gradient forces are unimportant so that dark matter and photons move together, we can determine these quantities from the Einstein equations without having to solve the coupled equations of motion for all the matter and radiation species. This is because, on scales larger than the acoustic length, the matter plus radiation behaves as a single fluctuating perfect fluid. The Einstein equations have built-in redundancy — they enforce local energy-momentum conservation — so we can use them to get the net energy density and velocity perturbations without having to solve the fluid equations. (That is a radical concept to a Newtonian physicist, but it is a direct consequence of the Einstein equations!)

From equation (19), dropping the curvature and Laplacian terms (they are both small on scales larger than the Hubble length) and neglecting anisotropic stress (i.e. setting $\phi = \psi$), we obtain

$$\frac{\delta\rho}{\bar\rho} = -2\left(a\partial_a\phi + \phi\right) = -2\partial_y(y\phi) \ . \tag{42}$$

Note that we are using a gravitational field equation to solve for the mass density perturbation, having used time-evolution equations to solve for the potential. By contrast, in Newtonian physics we are used to solving time evolution equations for the fluid variables and then solving a gravitational field equation for the potential. In general relativity, we have more flexibility in how to compute gravity.

Equation (42) has a simple physical interpretation. By assumption, the density is smoothly varying on scales of the Hubble length. Thus, each Hubble volume behaves like a homogeneous universe (slightly closed or slightly open depending on the sign of $\delta\rho$). In a homogeneous model, the density and cosmic proper time t measured by a fundamental observer are related by $\rho(x,\tau) \propto (Gt^2)^{-1}$. Because of the long-wavelength perturbations in g_{00}, however, the relative clock rate between proper time $t(x,\tau)$ and conformal time depends on position: $dt/d\tau = a(\tau)(1+\phi)$. Thus, we may write $t = t_0(\tau) + \Delta t(x,\tau)$

where $t_0(\tau) = \int a\, d\tau$ and $\Delta t = \int \phi a\, d\tau$. The density perturbation is computed at fixed τ using $\delta\rho/\bar{\rho} = (d\ln\rho/dt)\Delta t = -2(\Delta t)/t_0$. If $\partial_\tau \phi = 0$, then $\Delta t = \phi t_0$ giving $\delta\rho/\bar{\rho} = -2\phi$. This is simply the gravitational redshift: clocks run slower in a gravitational potential well.

If $\partial_\tau \phi \neq 0$, the gravitational redshift is time-dependent and a more careful calculation is needed. Matters are complicated because of the particular, somewhat arbitrary choice of constant-τ hypersurfaces implied by our metric equation (1). Our intuition is not always a good guide for physics on scales larger than the Hubble length. Fortunately, the Einstein equations will guide us to the correct solution even if we cannot guess it from Newtonian considerations.

The photon density perturbation on large scales follows simply from combining equation (42) with equation (34). (One must combine the photon and matter perturbations with appropriate weights to obtain the net density perturbation.) The result is

$$\delta_\gamma = \frac{9}{4} c_w^2 \left[-2(1+y)\partial_y(y\phi) + (2y/3)\tau_e^2 \nabla^2 \sigma \right] \ . \tag{43}$$

Similarly, the large-scale peculiar velocity follows from equation (20). For a matter plus radiation universe on scales much larger than the curvature and acoustic scales, $u_c = u_\gamma$. The velocity potential is then

$$u_\gamma = \frac{1}{2} \frac{y\sqrt{1+y}}{1+(3/4)y} \tau_e \partial_y(y\phi) \ . \tag{44}$$

6.1 Isentropic and Isocurvature modes

We now have all the ingredients needed to compute the CMB anisotropy on large angular scales. The treatment here is equivalent to that of Sachs & Wolfe (1967) for isentropic initial fluctuations and extends their treatment to more general initial conditions.

Equation (39) has two physically relevant quantities: the gravitational potential ϕ and specific entropy perturbation σ. Because the equation is second-order, one might think there are two physical solutions for any σ, and therefore a vast family of solutions. However, we have seen that σ cannot change with time over distance scales larger than the acoustic length. Moreover, there is only one combination of the homogeneous solutions of equations (41) that remains finite as $y \to 0$. Consequently, physical initial conditions set in the very early universe must be a linear combination of the finite solution with $\nabla^2\sigma = 0$ but $\phi \neq 0$ and of the finite solution with $\nabla^2\sigma \neq 0$ but $\phi = 0$. Because the evolution equations are all linear in the perturbations, then general solution is a linear combination of the solutions starting from these two types of initial conditions.

The two sets of solutions we have identified are called *isentropic* and *isocurvature*. In both cases we assume that the fluctuations are produced in the very early universe.

This assumption is consistent with inflation but not with some other models of structure formation where the density fluctuations are generated much later.

Isentropic fluctuations are defined by the condition $\sigma = 0$ but $\phi \neq 0$. They correspond to the energy density of all components (photons, baryons, dark matter, etc) varying together in such a way that the entropy perturbation vanishes. In particular, the photon-to-baryon number density ratio is a universal constant in this model (until after recombination, when photons and baryons decouple), as is the initial photon-to-dark matter particle number density ratio. This it exactly the condition resulting from standard inflation plus reheating. Inflationary fluctuations are often called "adiabatic" although isentropic (i.e. $\sigma = 0$ initially) is more accurate and descriptive.

Isocurvature fluctuations have $\phi = 0$ initially (i.e. no curvature perturbation) but $\sigma \neq 0$. Physically, they correspond to an equation of state $p(\rho, S)$ with spatially-varying entropy S but initially constant ρ. Isocurvature fluctuations can be created by a first-order phase-transition or any other process that produces spatial variations in the photon/baryon or photon-to-dark matter ratio while leaving the net energy density unperturbed. As the universe expands, as long as particle collisions are rapid, the specific entropy of each fluid element is conserved. That is, prior to decoupling for any particle species, the ratio of number densities of that particle to photons is conserved. If the ratio varies spatially, then pressure gradients develop which move matter and cause a gravitational potential perturbation to develop. Nonstandard models of inflation can be constructed in which entropy perturbations are generated during or after reheating.

In our particular case we are considering "isocurvature CDM" perturbations, since $\sigma \neq 0$ corresponds to a spatially varying photon-to-CDM ratio in equation (33). It is also possible to consider models with a fixed T_γ^3/ρ_c but with spatially varying T_γ^3/ρ_b, or "isocurvature baryon" models. Indeed, isocurvature-type perturbations can be produced that have the ratio of any two or more species varying in space initially, as long as the total energy density is constant so that the metric is unperturbed ($\phi = 0$).

It is easy to recognize the isentropic and isocurvature "modes" (as they are often called in the literature) as homogeneous and particular solutions of equation (39). We impose initial conditions at $\tau = \tau_i$ such that $y_i \ll 1$. Isentropic initial conditions have $\phi(x, \tau_i) = \phi_i(x)$ and $\sigma(x, \tau_i) = \partial_\tau \phi(x, \tau_i) = 0$. (For example, the fluctuations produced by inflation are frozen in and unchanging during the radiation-dominated era on scales larger than the acoustic length.) Isocurvature initial conditions have $\phi(x, \tau_i) = \partial_\tau \phi(x, \tau_i) = 0$ and $\sigma(x, \tau_i) = \sigma_i(x)$, with $\partial_\tau \sigma = 0$ on scales larger than the acoustic length.

We leave it as an exercise for the student to show that the desired solutions of equation (39) are

$$\phi(x, \tau) = \begin{cases} \frac{9}{10}\phi_1(y)\phi_i(x) \ , & \text{isentropic ;} \\ \frac{2y}{5(4+3y)}\phi_1(y)\tau_e^2\nabla^2\sigma_i(x) \ , & \text{isocurvature .} \end{cases} \tag{45}$$

(The ϕ_2 solution is not included here because it is the decaying mode. Its amplitude

must be negligible at late times because ϕ_2 diverges as $y \to 0$.) In the matter-dominated era, $y \gg 1$, the general solution including both isentropic and isocurvature modes is a constant potential,

$$\phi(x,\tau) \approx \frac{9}{10}\phi_i(x) + \frac{1}{5}\left(\frac{2}{3}\tau_e^2\nabla^2\sigma_i\right) \quad \text{for } y \gg 1 \ . \tag{46}$$

The entropy term in parentheses is simply the relative variation of the photon-to-CDM ratio from equation (34). The relative sizes of the coefficients in equation (46) (0.9 vs 0.2) shows how inefficient entropy is in producing a gravitational potential fluctuation. This will cause the isocurvature mode to have a much larger CMB anisotropy than the isentropic mode, for a given post-recombination gravitational potential.

The Sachs-Wolfe anisotropy follows from substituting into equations (12) and (18) the potential, density and velocity perturbations computed on large scales assuming that recombination occurs at $y \gg 1$. First, from equations (18), (43), (44), and (46), we get

$$\Delta_{\rm e} = \begin{cases} -(2/3)\phi_{\rm e} - (2/3\eta_{\rm e})n^i\nabla_i\phi_{\rm e} \ , & \text{isentropic ;} \\ \phi_{\rm e} - (2/3\eta_{\rm e})n^i\nabla_i\phi_{\rm e} \ , & \text{isocurvature ,} \end{cases} \tag{47}$$

where $\eta_e \equiv (\dot{a}/a)_{\rm e}$ and subscript e refers to recombination. Note that the velocity term becomes small for comoving wavelengths much larger than the Hubble distance $\eta_{\rm e}^{-1}$ at recombination. Note also the critical difference between isentropic and isocurvature initial conditions as far as the post-recombination potential. Combining equation (12 with (47), we get the final Sachs-Wolfe effect for the anisotropy in direction (θ,φ):

$$\Delta(\theta,\varphi) = \left(C + \frac{2}{3\eta_{\rm e}}\frac{\partial}{\partial\chi}\right)\phi(\chi_{\rm e},\theta,\varphi,\tau_{\rm e}) + 2\int_0^{\chi_{\rm e}} d\chi\,\partial_\tau\phi(\chi,\theta,\varphi,\tau_0-\chi) \ , \tag{48}$$

where $C = 1/3$ for isentropic fluctuations and $C = 2$ for isentropic fluctuations. Note that equation (48) includes only the gravitational potential at and after recombination — by ignoring all acoustic effects (and neutrinos) we have simplified the evolution sufficiently to express the primary anisotropy entirely in terms of the potential and its derivatives for $\tau \geq \tau_{\rm e}$. To the extent that the first two terms (intrinsic and Doppler anisotropy) dominate the anisotropy, maps of the CMB anisotropy reveal (on scales larger than the acoustic horizon) the gravitational potential at recombination.

The coefficient C is six times larger for isocurvature fluctuations than for isentropic ones. (This is, of course, an approximation — the solution assumed $z_{\rm rec} \ll z_{\rm eq}$ which is not exact.) For a given amplitude of gravitational potential fluctuations, hence dark matter fluctuations (dark matter being the dominant component at recombination), isocurvature fluctuations produce a much larger CMB anisotropy. This is because the initial entropy fluctuations directly perturb the radiation with no compensating time dilation

effect. For isentropic fluctuations, we saw that the large-scale photon density perturbation has opposite sign to the gravitational potential (because of the time dilation effect discussed following eq. 42), which results in a cancellation of the CMB anisotropy. Hence the famous Sachs-Wolfe formula $\Delta = \frac{1}{3}\phi$. Although Sachs & Wolfe (1967) did not consider isocurvature initial conditions, we have seen that it is just as easy to estimate their contribution to large-scale anisotropy. The much larger ratio of CMB fluctuations to dark matter perturbations has led to a rejection of most isocurvature models.

7 Green's function solution for small-scale anisotropy

As we have seen, the coupled Einstein and fluid equations can be solved analytically on large scales, with the result that the temperature anisotropy basically traces the gravitational potential fluctuations on the CMB photosphere. However, this is not the full story for CMB anisotropy. On smaller scales, the potential fluctuations set the photon-baryon fluid into motion, sending sound waves propagating through the universe. These sound waves leave a characteristic signature in the correlations of CMB anisotropies on angular scales of about one degree. This signature is reflected in the acoustic peaks of the angular power spectrum.

On scales smaller than the acoustic length, it is hard to solve the coupled Einstein and fluid equations for a multicomponent medium. The usual procedure is to work in Fourier space so that the partial differential equations become ordinary differential equations in time. Seljak (1994) solved equations (29) and (20) numerically in Fourier space. Ma & Bertschinger (1995) solved the complete coupled system including the Boltzmann equation for photons and neutrinos, which are necessary for imperfect fluids or collisionless plasmas. Seljak & Zaldarriaga (1996) introduced CMBFAST, a fast computer code for solving the complicated system of equations. These developments are valuable, especially CMBFAST because it has revolutionized CMB data analysis and model testing.

Here, however, we seek physical insight more than numerical results. The approach is based on work by Sergei Bashinsky (Bashinsky 2001, Bashinsky & Bertschinger 2001, 2002). Instead of solving the fluid and Einstein equations in Fourier space, we solve the coupled wave equations (31) and (37) in configuration space (x, τ).

Our model for CMB anisotropy is based on two fluids coupled by gravity: the photon-baryon fluid (with sound speed $c_{\rm s}$) and CDM (with vanishing sound speed). On physical grounds, we would expect waves to propagate through the photon-baryon fluid with speed $c_{\rm s}$ but no waves to propagate through the CDM. It is intriguing that equations (31) and (37) have almost the expected form, namely a coupled system of damped wave equations with the appropriate sound speeds. However, the fundamental variables appearing there are the gravitational and entropy potentials, which do not cleanly separate the two fluids.

If we ignore curvature by setting $K = 0$ (as is justified at high redshift), then the

Laplacian operators in equations (31) and (37) both operate on the same quantity, namely $\phi + \sigma/y$. This suggests that we consider linear combinations of ϕ and σ to separate the wave components. Amazingly, there is a simple set of variables that does the trick:

$$\phi_r = \left(\frac{c_w}{c_{\rm s}}\right)^2 \left(\phi + \frac{\sigma}{y}\right) \ , \quad \phi_c = \phi - \phi_r \ . \tag{49}$$

We use the subscripts r for radiation (the photon-baryon fluid, with an approximate inclusion of neutrinos) and c for CDM. The reason for doing so is that the Poisson equation now holds separately for each potential with a corresponding source (for $K = 0$):

$$\begin{aligned} \nabla^2\phi_r &= 4\pi G a^2 \bar\rho_r \left(\delta_\gamma + 3\frac{\dot a}{a}\bar u\right) \ , \\ \nabla^2\phi_c &= 4\pi G a^2 \bar\rho_c \left(\delta_c + 3\frac{\dot a}{a}\bar u\right) \ , \end{aligned} \tag{50}$$

where

$$\bar u \equiv \frac{\bar\rho_r u_\gamma + \bar\rho_c u_c}{\bar\rho_r + \bar\rho_c} \ , \quad \bar\rho_r \equiv \frac{4}{3}(\bar\rho_\gamma + \bar\rho_\nu) + \bar\rho_b \ . \tag{51}$$

Thus, we may interpret ϕ_r as the gravitational potential produced by "radiation" (photons, neutrinos, and baryons) while ϕ_c is the gravitational potential produced by CDM. (One must be careful not to push the Newtonian analogy too far, since here we have contributions from the peculiar velocity potentials.) Equations (50) are equivalent to equation (22) applied separately to each of our two fluids.

Equations (31) and (37) now separate into a pair of coupled wave equations with the expected behavior:

$$\begin{aligned} \partial_\tau^2\phi_r + 3(1+c_{\rm s}^2)\frac{\dot a}{a}\,\partial_\tau\phi_r + 3c_w^2\frac{\dot a}{a}\,\partial_\tau\phi_c + \frac{3(c_w^2+\varphi)}{4\tau_e^2 y}\,\phi_r - \frac{2c_{\rm s}^{-2} - 4 + 3c_w^2}{3\tau_e^2 y^2}\,\phi_c &= c_{\rm s}^2\nabla^2\phi_r \ , \\ \partial_\tau^2\phi_c + 3(c_w^2 - c_{\rm s}^2)\frac{\dot a}{a}\,\partial_\tau\phi_r + 3\frac{\dot a}{a}\,\partial_\tau\phi_c - \frac{3\varphi}{4\tau_e^2 y}\,\phi_r + \frac{2c_{\rm s}^{-2} - 3}{3\tau_e^2 y^2}\,\phi_c = 0 \ , \end{aligned} \tag{52}$$

where $\varphi(y)$ is a ratio of two quartic polynomials given by Bashinsky & Bertschinger (2002).

The first of equations (52) shows that perturbations in the photon-baryon fluid indeed propagate as sound waves with speed $c_{\rm s}$. As the sound wave passes by a CDM fluid element, its gravity acts on the CDM, causing the CDM to evolve as given by the second equation.

7.1 Radiation era

Equations (52) are still too complicated to solve analytically. To gain insight, let us examine the solutions in the radiation era, $y \ll 1$. In this limit, equations (52) become

$$\begin{aligned} \partial_\tau^2 \phi_r + \frac{1}{\tau}\,\partial_\tau(4\phi_r + \phi_c) - \frac{1}{\tau^2}\,\phi_c &= c_{\rm s}^2 \nabla^2 \phi_r \ , \\ \partial_\tau^2 \phi_c + \frac{3}{\tau}\,\partial_\tau \phi_c + \frac{1}{\tau^2}\,\phi_c &= \frac{3}{4}(y - y_b)\left(\frac{1}{\tau}\,\partial_\tau \phi_r + \frac{4}{\tau^2}\phi_r\right) \ . \end{aligned} \tag{53}$$

We will solve these for isentropic initial conditions, $\sigma = 0$ as $y \to 0$. From equations (49), $\phi_c/\phi_r \propto y$. Thus, CDM has negligible effect on the dominant radiation component in the radiation era. On the other hand, the radiation perturbations provide the source for ϕ_c.

Thus, we must solve the simple damped wave equation

$$\partial_\tau^2 \phi_r + \frac{4}{\tau}\,\partial_\tau \phi_r = c_{\rm s}^2 \nabla^2 \phi_r \tag{54}$$

with constant sound speed $c_{\rm s} = 3^{-1/2}$. Since this is a partial differential equation, we must specify the initial conditions for all space. However, the problem simplifies because it is a linear partial differential equation. The linear superposition principle means that we can expand the solution in any convenient set of spatial basis functions. The common choice in cosmology for flat (Euclidean) space is the plane wave basis $\exp(i\vec{k}\cdot\vec{x}\,)$, so that $\nabla^2 = -k^2$ for any given plane wave component. We use the usual notation of flat space in which $\vec{k}$ and $\vec{x}$ are 3-vectors.

The Fourier space solution to equation (54) is

$$\phi_r(k,\tau) = 3\,\frac{j_1(k\tau)}{k\tau} \ , \tag{55}$$

where $j_1(x) = (\sin x - x\cos x)/x^2$ is a spherical Bessel function. Note that the normalization chosen so that $\phi_r = 1$ for $\tau = 0$.

Suppose that the initial potential fluctuations at the end of the inflationary era are $\phi_i(\vec{x}\,)$. The Fourier transform is $\phi_i(\vec{k}\,)$. (Note the common practice of using the same function name to denote the real-space function and its Fourier transform. The meaning becomes clear from the argument: $\vec{x}$ is always a spatial position and $\vec{k}$ is always a wavevector.) Linear superposition means that the Fourier transform at any later time is

$$\phi_r(\vec{k},\tau) = \phi_r(k,\tau)\phi_i(\vec{k}\,) \tag{56}$$

By analogy with linear filters in electrical systems, $\phi_r(k,\tau)$ is called the *transfer function* for the radiation potential. It is the factor by which every Fourier component of $\phi_r(\vec{k},\tau)$

changes through linear evolution. Every linear field has a transfer function (e.g. ϕ_c, δ_γ, etc.). The transfer function is spherically symmetric in $\vec{k}$-space because of the rotational invariance of the equations of motion. Note carefully the notation: $\phi_r(k,\tau)$ is the transfer function, i.e. the solution subject to initial condition $\phi_r = 1$, while $\phi_r(\vec{k},\tau)$ is the solution subject to the initial condition $\phi_r = \phi_i(\vec{k}\,)$. The point is that once the transfer function is known, then the solution for arbitrary initial condition follows by simple multiplication.

The transfer function is the solution to the evolution equation with initial condition $\exp(i\vec{k}\cdot\vec{x}\,)$. Plane wave initial conditions are but one possible choice of initial condition. Another useful choice is a point-like perturbation at the origin,

$$\phi_r^{(3)}(\vec{x},\tau) \to \delta_{\rm D}^{(3)}(\vec{x}\,) \quad \text{as } \tau \to 0 \tag{57}$$

where $\delta_{\rm D}^{(3)}(\vec{x}\,)$ is the three-dimensional Dirac delta function. The superscript (3) is placed on ϕ_r to remind us that the initial condition is point-like in three dimensions.

The solution subject to a point-like initial condition is called a Green's function. The solution at any later time is then simply a convolution of the initial field by the Green's function:

$$\phi_r(\vec{x},\tau) = \int d^3x'\, \phi_r(\vec{x}\,',0)\phi_r^{(3)}(\vec{x}-\vec{x}\,',\tau)\ . \tag{58}$$

Heuristically, we can imagine decomposing the initial field into a sum of delta functions. Each delta function evolves into the Green's function. The evolved field is therefore a superposition of Green's functions.

The Green's function description is mathematically equivalent to the Fourier space description with a transfer function. In fact, the Green's function is simply the inverse Fourier transform of the transfer function:

$$\phi(k,\tau) = \int \phi^{(3)}(r,\tau)\, e^{-i\vec{k}\cdot\vec{x}}\, d^3x\ . \tag{59}$$

(We remove the subscript r since this relation is not restricted to the radiation potential but is true for any transfer function and Green's function pair.) Note that since the transfer function is spherically symmetric in k-space, the Green's function is also spherically symmetric in position space. That is, $\phi^{(3)}$ depends only on the length $r = |\vec{x}\,|$. (Assuming a flat cosmology, we use r interchangeably with the radial comoving coordinate χ.) The spherical Green's function and transfer function are Fourier transform pairs.

In the Fourier domain, the evolved field follows by multiplication with the transfer function. In the position domain, the evolved field follows by convolution with the Green's function. The Fourier transform of a convolution is the product of Fourier transforms, and the Fourier transform of a product becomes a convolution.

So what is the Green's function corresponding to the radiation transfer function $\phi_r(k,\tau)$? It is easily found either by Fourier transformation of equation (55) or by

solution of equation (54) in spherical coordinates with delta function initial condition. The result is

$$\phi_r^{(3)}(r,\tau) = \frac{3}{4\pi}(c_s\tau)^{-3}\theta(c_s\tau - r) \tag{60}$$

where $\theta(x)$ is the Heaviside step function, $\theta(x) = 0$ for $x < 1$ and $\theta(x) = 1$ for $x > 1$.

The Green's function for the radiation potential is remarkably simple: it is a spatially uniform wave expanding at the speed of sound, with unit volume integral (from eq. 59 for $k = 0$). In short, it is a spherical sound wave! The oscillations of the transfer function $3j_1(k\tau)/(k\tau)$ arise because of the finite extent of the Green's function and they are characteristic of causal behavior. This phenomenon is essentially the origin of the acoustic peaks of the CMB power spectrum, which we will discuss below.

This beautifully simple result suggests that we apply the Green's function method to the full problem of equations (52) for all times. However, there is a practical problem with the three-dimensional Green's functions. The Poisson equation tells us that the photon density fluctuation δ_γ is given, in part, by $\nabla^2\phi_r^{(3)}$. The derivative of the Heaviside function is a Dirac delta function. The Laplacian takes one more derivative, so that $\delta_\gamma^{(3)}(r,\tau)$ has a term proportional to $d\delta_D(r - c_s\tau)/dr$. Great care must be exercised when dealing with derivatives of delta functions, especially when $\phi_r^{(3)}$ is determined numerically. The numerical challenges are serious enough to dissuade us from using three-dimensional Green's functions.

These delta function singularities are a consequence of the perfect fluid assumption. If photon diffusion is included, then the acoustic wavefront will spread slightly. Even with diffusion, however, the spherical transfer function for δ_γ is sharply peaked at the radius of the acoustic sphere. This means that an initial point-like perturbation in the potential, located on or near the CMB photosphere, will produce a ring of temperature anisotropy on the sky. The observed pattern is a superposition of such rings like the ripples from stones dropped in a pond. The maximum size of the rings — twice the acoustic radius at recombination — imprints a characteristic scale in the CMB anisotropy.

7.2 Plane-parallel Green's functions

For numerical integration purposes it is preferable to modify the Green's function method to avoid derivatives of delta functions. The singular behavior is reduced if we superpose many spherical waves to create a plane wavefront using the Huyghens' construction. This works for any Green's function as follows:

$$\phi^{(1)}(x,\tau) = \int_{|x|}^{\infty} \phi^{(3)}(r,\tau)\, 2\pi r dr \ . \tag{61}$$

The integral ensures that $\phi^{(1)}$ is less singular than $\phi^{(3)}$ at the wavefronts. From equation (59) it follows that $\phi^{(1)}$ is the one-dimensional inverse Fourier transform of the transfer

function,

$$\phi(k,\tau) = \int_{-\infty}^{\infty} \phi^{(1)}(x,\tau)\, e^{-ikx}\, d^3x \tag{62}$$

where $r = |\vec{x}\,|$. The transfer function contains the same information as either its one-dimensional or three-dimensional Fourier transform. Thus, the choice of approach is purely a matter of convenience, numerical ease or accuracy, and/or ease of interpretation.

Recalling the initial condition $\phi(k,0) = 1$ for the transfer function, from equation (62) it follows that $\phi^{(1)}(x,\tau)$ is the Green's function for initial condition $\phi(\vec{x},0) = \delta_{\rm D}(x)$. The initial perturbation is sheet-like (i.e., constant on planes of constant Cartesian coordinate x) rather than point-like. We use the superscript (1) to distinguish such plane-parallel Green's functions from the spherical variety.

Analytic solutions for the plane-parallel Green's functions in the radiation era are given by Bashinsky & Bertschinger (2002). Because the dynamics involve two potentials (for gravity and entropy), initial conditions must be set for both. The calculations have all assumed isentropic initial conditions with $\sigma(x,\tau) = 0$ at $\tau = 0$. It would be interesting to work out Green's functions for isocuravture initial conditions with $\phi(x,0) = 0$ and $\sigma(x,0) \propto 1/r$ (so that the entropy perturbation $\nabla^2\sigma$ is a delta function) but this has not been done.

Bashinsky (2001) constructed numerical solutions for the isentropic case by evolving equations (52) in one space dimension and time, with $\nabla^2 = \partial^2/\partial x^2$. Usually it is much harder to accurately solve partial differential equations than ordinary differential equations, and this is an argument for the Fourier space approach. However, the equations in question are linear wave equations and they may be solved by the method of characteristics. This method is fast and accurate.

Figure 1 shows the results of this numerical integration for the radiation and CDM gravitational potentials at recombination. The initial conditions were $\phi_r^{(1)}(x,0) = \delta_{\rm D}(x)$ and $\phi_c^{(1)}(x,0) = 0$. The delta function separated into left-going and right-going waves, whose evolution spread $\phi_r^{(1)}$ over space and diminished the central peak. The gravitational potential hill of the radiation caused outward-directed gravitational forces which expelled the CDM away from $x = 0$. The CDM has a central cusp reflecting the initial repulsive singularity in the gravitational potential $\phi_r^{(1)}$; this cusp is preserved because the CDM particles have no thermal motion. In fact, once the universe becomes matter-dominated $\phi_c^{(1)}(x,\tau)$ stops evolving, as may be seen from the second of equations (52) in the limit $y \gg 1$.

Figure 2 shows three snapshots of the time evolution of the Green's functions for the radiation and CDM potentials. Only the range $x > 0$ needs to be plotted since the Green's functions depend only on $|x|$. Note that while the amplitude of ϕ_r decreases rapidly with time, ϕ_c changes much more slowly and becomes constant in the matter era as expected. We also see the effect of changing the baryon content. This changes the photon-baryon sound speed in equation (28), thereby changing the distance to the

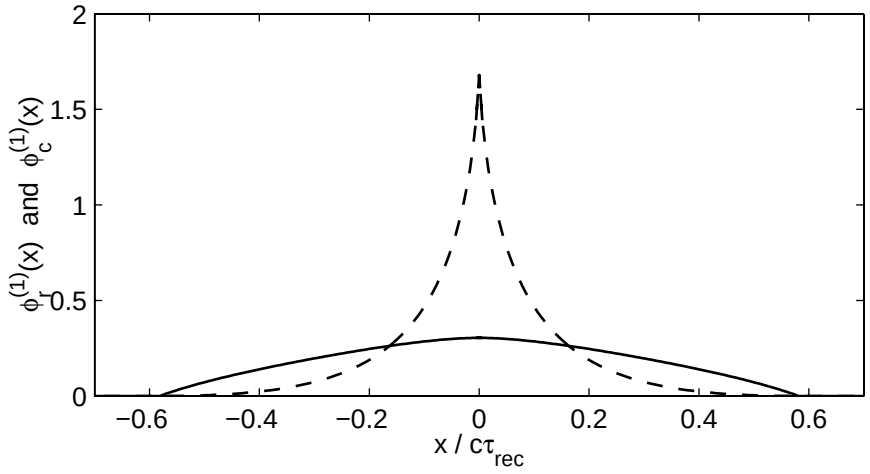

Figure 1: Plane-parallel Green's functions for the potentials ϕ_r (solid) and ϕ_c (dashed) at recombination, in the fluid approximation. The cosmological parameter values are $\Omega_{\rm m} = 0.35$, $\Omega_\Lambda = 0.65$, $\Omega_b h^2 = 0.02$, and $h = 0.65$. By recombination the universe has become matter-dominated. From Bashinsky (2001).

wavefront. Adding baryons decreases the sound speed.

The density and velocity perturbations of photons, baryons, and the CDM fluid follow from ϕ_r, ϕ_c and their derivatives. The photon perturbations contribute directly to CMB anisotropy while the CDM perturbations eventually seed the formation of galaxies. Figure 3 shows the plane-parallel Green's functions at recombination for the photon and CDM density fluctuations. (Recall that $\delta_b = \delta_\gamma$ in the fluid approximation.) The singularities of δ_γ and δ_c arise from the $d^2\phi/dx^2$ term of the Poisson equation. Comparing with Figure 1, we see why these singularities occur at the wavefronts for δ_γ but at $x = 0$ for CDM. The central spike for the CDM is negative because of the repulsive sign of the initial gravitational potential peak (top row of Fig. 2). It is surrounded by positive tails because of mass conservation: the CDM pushed out from $x = 0$ piles up into the region between $x = 0$ and the acoustic wavefront.

Note from Figures 1–3 that our spacetime is unperturbed outside of the acoustic wavefront. This is a consequence of our initial condition that left the metric unperturbed everywhere except at $x = 0$. Had we instead made δ_γ a Dirac delta function with zero velocity perturbation, then the gravitational potential ϕ would have been nonzero for all x. However, our treatment in the earlier sections shows that the gravitational potential, not the density, is the fundamental physical quantity for CMB anisotropy. That is why our Green's functions are chosen so that $\phi(x, 0) = \delta_{\rm D}(x)$.

The Dirac delta function contributions of $\delta_\gamma(x, \tau)$ at the acoustic wavefronts make

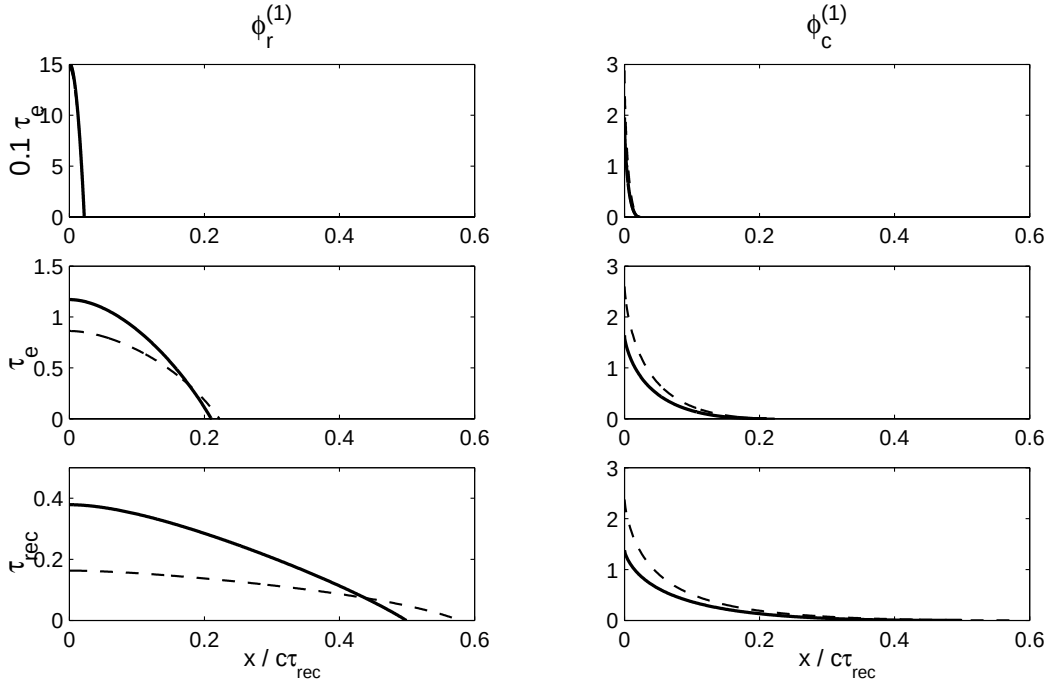

Figure 2: Time evolution of the plane-parallel Green's functions for the potentials ϕ_r (left) and ϕ_c (right) in the fluid approximation. The solid (dashed) lines show the results for $\Omega_b h^2 = 0.03$ ($\Omega_b h^2 = 0$). The three rows give snapshots at the times ($0.1\tau_e$, τ_e, and $\tau_{\rm rec} = 2.5\tau_e$). The speed of sound is decreased below $c/\sqrt{3}$ by the inclusion of baryons. From Bashinsky (2001).

a significant contribution to the total CMB anisotropy. So does the dip at $x = 0$. To understand the physics of this dip, let us examine the combination of photon density and gravitational potential appearing in the Sachs-Wolfe effect on large scales, which is given by equation (48) without the Doppler and $\partial_\tau \phi$ (integrated Sachs-Wolfe) contributions:

$$\Delta_{\rm eff} \equiv \frac{1}{3}\,\delta_\gamma + \phi\ . \tag{63}$$

(Recall that δ_γ is defined here as the fractional perturbation in photon number density.) The plane-parallel Green's function for $\Delta_{\rm eff}$ at recombination is shown in Figure 4. Note that the relation of $\Delta_{\rm eff}$ to potential on small scales in position space is quite different from the $\Delta_{\rm eff} \approx \frac{1}{3}\phi$ of the large-scale Sachs-Wolfe effect. However, this relation still holds if one integrates the Green's functions over x to get the long wavelength contributions. The positive Dirac delta functions more than compensate for the negative $\delta_\gamma(x)$ behind the acoustic wavefronts so that $\int \Delta_{\rm eff}(x)\,dx \approx \frac{1}{3}\int(\phi_r + \phi_c)\,dx$.

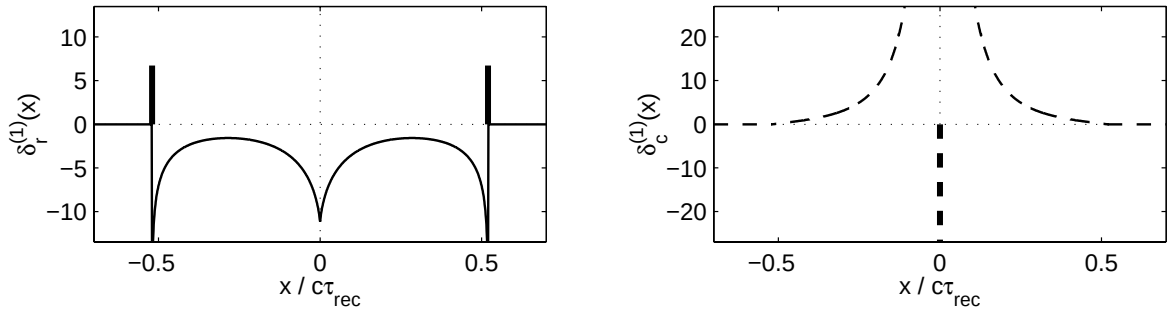

Figure 3: Plane-parallel Green's functions for the density fluctuations of photons ($\delta_r = \delta_\gamma$, solid) and CDM (dashed) at recombination, in the fluid approximation, for the same parameters shown in Fig. 1. Thick vertical lines represent Dirac delta functions of $\delta_\gamma(x)$ at its acoustic wavefronts and of $\delta_c(x)$ at the origin. From Bashinsky (2001).

Figure 4 suggests that baryons are responsible for the central dip in $\Delta_{\rm eff}$. This dip is easy to understand. From Figure 1, the total gravitational potential has a sharp peak at $x = 0$. The photon-baryon fluid has a high sound speed and therefore quickly adjusts to this potential by settling into hydrostatic equilibrium near $x = 0$. (Obviously hydrostatic equilibrium does not apply at the acoustic wavefronts, but it does hold as $x \to 0$ where the elapsed time is many sound-crossing times.) From the second of equations (25) we obtain the equation of hydrostatic equilibrium,

$$\nabla_i \rho + (\rho + p) \nabla_i \phi = 0 \ . \tag{64}$$

Linearizing this for the photon-baryon fluid gives

$$\nabla_i \left[\frac{1}{4} \delta_\gamma + \left(1 + \frac{3}{4} \frac{\bar\rho_b}{\bar\rho_\gamma} \right) \phi \right] = \nabla_i \left(\Delta_{\rm eff} + \frac{3}{4} \frac{\bar\rho_b}{\bar\rho_\gamma} \phi \right) = 0 \ . \tag{65}$$

Thus, if $\rho_b = 0$, $\Delta_{\rm eff}$ has zero gradient in hydrostatic equilibrium. If $\Omega_b \neq 0$, on the other hand, $\Delta_{\rm eff}(0, \tau) = -\frac{3}{4}(\bar\rho_b / \bar\rho_\gamma)\phi + \text{constant}$ as $x \to 0$. The positive cusp of the CDM potential becomes a negative cusp of CMB anisotropy whose amplitude is proportional to Ω_b. Thus, baryons have two main effects on CMB anisotropy: they slow the sound speed and thereby decrease the acoustic distance compared with a pure photon gas, and they create a central dip in the Green's function.

8 Angular Power Spectrum

The goal of CMB integrations is to predict the anisotropy in a given cosmological model. We must ask carefully what this means. Does it mean to predict the actual pattern of

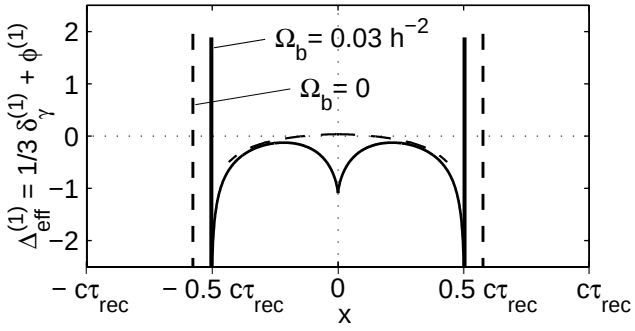

Figure 4: Plane-parallel Green's function for the combined intrinsic ($\frac{1}{3}\delta_\gamma$) plus gravitational redshift contributions to CMB anisotropy at recombination in the fluid approximation, for the same parameters as shown in Fig. 2. The solid (dashed) lines show the results for $\Omega_b h^2 = 0.03$ ($\Omega_b h^2 = 0$). The quantity $\Delta_{\rm eff}$ not only gives the Sachs-Wolfe contribution to CMB anisotropy on large scales, it also measures the departure of the photon-baryon fluid from hydrostatic equilibrium. Based on Bashinsky & Bertschinger (2001).

fluctuations that will be measured in the sky? No. That is impossible because the fluctuations originate from random fluctuations in the early universe (quantum fluctuations during inflation or perhaps thermal fluctuations in some first-order phase transition). At best, we can predict only the statistical properties of the CMB anisotropy. But then *what* statistical properties should we calculate?

Inflation predicts a gaussian random field of primeval potential fluctuations. That is, in a Fourier decomposition (here assuming a $K = 0$ background)

$$\phi(\vec{x},\tau) = \int d^3k\, e^{i\vec{k}\cdot\vec{x}}\, \phi(\vec{k},\tau)\ , \tag{66}$$

each mode $\phi(k)$ is a zero-mean, normally distributed random variable. Actually, the Fourier transform of a real field is a complex field, so each mode is a pair of normally distributed variables with the same variance. Also note that our definition of the Fourier transform here differs from that in equation (59).

For a Gaussian random field, the two-point correlation, i.e. the covariance of field values at different points, completely characterizes the statistical properties of the field. For $\phi(k)$, its covariance defines the power spectrum (or spectral density) $P_\phi(k)$:

$$\left\langle \phi(\vec{k})\phi^*(\vec{k}\,')\right\rangle \equiv P_\phi(k)\,\delta_{\rm D}(\vec{k}-\vec{k}\,')\ . \tag{67}$$

Had we used the alternative Fourier transformation definition implied by equation (59), the right-hand side would be larger by a factor $(2\pi)^3$. Note the three-dimensional Dirac

delta function $\delta_{\rm D}$. The complex conjugation may be removed provided that the argument of the delta function is changed to $\vec{k} + \vec{k}'$.

It is easy to check that the spatial covariance, i.e. the two-point correlation function, is the Fourier transform of the power spectrum:

$$\langle \phi(\vec{x}_1)\phi(\vec{x}_2)\rangle = \int d^3k\, e^{i\vec{k}\cdot(\vec{x}_1-\vec{x}_2)}\, P_\phi(k)\ . \tag{68}$$

Note that the correlations of different points in space are generally nonzero — in particular, scale-invariant fluctuations are a statistical fractal, with correlations extending over all scales — but that the correlation at different points vanishes in k-space because of the Dirac delta function in equation (67). This is a general feature of "stationary" random fields, i.e. random fields whose statistical properties are invariant under spatial translation. It is a natural outcome of inflationary models, where the fluctuations are the zero-point fluctuations of a nearly massless free field; each mode is independent.

Our calculations have shown that the primary CMB anisotropy Δ is linear in the gravitational potential (and its derivatives and integrals). Thus, the anisotropy at any point in the sky is a linear combination of gaussian-distributed random numbers. A linear combination of normal (gaussian) random numbers is itself normal. Thus, the anisotropy $\Delta_0(\vec{n})$ should be a gaussian random field on the sphere. Thus, to fully characterize its statistical properties we need only to calculate the analogue of the power spectrum on a sphere.

The angular power spectrum is straightforward to define by analogy with equations (66) and (67). We first expand the temperature anisotropy in the orthonormal basis functions appropriate for a sphere, spherical harmonics:

$$\Delta_0(\vec{n}) = \sum_{l=0}^{\infty}\sum_{m=-l}^{l} a_{lm}Y_{lm}(\vec{n}) \tag{69}$$

where $Y_{lm}(\vec{n})$ is shorthand for $Y_{lm}(\theta,\varphi)$ for spherical angles (θ,φ) giving the observational direction $\vec{n}$. (Note that here we are defining $\vec{n}$ to have opposite sign to the rest of these notes, for consistency with usage by experimentalists: $-\vec{n}$ is the direction the photon travels.) The angular power spectrum is now defined by the covariance of the expansion coefficients:

$$\langle a_{lm}a^*_{l'm'}\rangle \equiv C_l\,\delta_{ll'}\,\delta_{mm'} \tag{70}$$

where $\delta_{ll'}$ is now the Kronecker delta. Each angular coefficient is independent for a random field with rotational invariance on a sphere. This is the angular analogue to translational invariance, which led to a Dirac delta function in equation (67). The compactness of the sphere makes the sum over harmonics discrete rather than continuous, leading to a Kronecker delta rather than a Dirac delta function.

The angular analogue of equation (68) is the angular correlation function

$$C(\theta) \equiv \langle \Delta(\vec{n}_1)\Delta(\vec{n}_2)\rangle = \frac{1}{4\pi}\sum_{l=0}^{\infty}(2l+1)C_l P_l(\vec{n}_1\cdot\vec{n}_2) \tag{71}$$

where $\vec{n}_1\cdot\vec{n}_2 = \cos\theta$ and $P_l(x)$ is the Legendre polynomial of degree l. Notice that the angular correlation function $C(\theta)$ and power spectrum C_l are Fourier-Legendre transformations of each other and therefore contain the same information.

To calculate the angular power spectrum we must relate the anisotropy to the potential in k-space. We do this by expanding the anisotropy in plane waves. In the Sachs-Wolfe approximation, from equation (48) we get

$$\Delta_0(\vec{n}) = \int d^3k\,\left[e^{-i\chi_{\rm e}\vec{k}\cdot\vec{n}}\left(C - \frac{2i\vec{k}\cdot\vec{n}}{3\eta_{\rm e}}\right)\phi(\vec{k},\tau_{\rm e}) + 2\int_0^{\chi_{\rm e}} d\chi\, e^{-i\chi\vec{k}\cdot\vec{n}}\,\partial_\tau\phi(\vec{k},\tau_0-\chi)\right] \tag{72}$$

with $C \approx \frac{1}{3}$ for the isentropic mode and $C \approx 2$ for isocurvature modes. The minus sign in the plane waves occurs because $-\vec{n}$ is the radial unit vector.

Now we use the spherical wave expansion of a plane wave,

$$e^{ix\mu} = \sum_{l=0}^{\infty} i^l(2l+1)j_l(x)P_l(\mu) \tag{73}$$

where $j_l(x)$ is the spherical Bessel function (e.g. Jackson *Classical Electromagnetism*). Substituting into equation (72) yields

$$\Delta_0(\vec{n}) = \int d^3k\sum_{l=0}^{\infty}(-i)^l(2l+1)\Delta_l(\vec{k},\tau_0)P_l(\hat{k}\cdot\vec{n}) \tag{74}$$

where $\hat{k} = \vec{k}/k$ and, in the Sachs-Wolfe approximation,

$$\Delta_l(\vec{k},\tau_0) = \left[Cj_l(k\chi_{\rm e}) + \frac{2}{3\eta_{\rm e}}j_l'(k\chi_{\rm e})\right]\phi(\vec{k},\tau_e) + 2\int_0^{\chi_{\rm e}} d\chi\, j_l(k\chi)\,\partial_\tau\phi(\vec{k},\tau_0-\chi)\ . \tag{75}$$

(The derivative term j_l' came from differentiating eq. 73 with respect to x, which brings down the factor $i\mu = -i\hat{k}\cdot\vec{n}$ needed for the Doppler term in eq. 72.)

We need one more mathematical result, the addition theorem for spherical harmonics,

$$P_l(\vec{n}_1\cdot\vec{n}_2) = \frac{4\pi}{2l+1}\sum_{m=-l}^{l} Y_{lm}(\vec{n}_1)Y_{lm}^*(\vec{n}_2)\ . \tag{76}$$

Using equations (69), (74), and (76), we obtain

$$a_{lm} = (-i)^l 4\pi\int d^3k\, Y_{lm}^*(\hat{k})\,\Delta_l(\vec{k},\tau_0)\ . \tag{77}$$

To get the angular power spectrum we must now relate the potentials in equation (75) to the initial random field of potential or entropy fluctuations that induced the CMB anisotropy. We define the CMB *transfer function*

$$D_l(k) \equiv \frac{\Delta_l(\vec{k}, \tau_0)}{\phi_i(\vec{k})} \tag{78}$$

where $\phi_i(\vec{k})$ is the Fourier transform of the primeval potential field of equation (46). (This assumes the initial fluctuations were isentropic; if they were isocurvature, then ϕ_i should be replaced by the initial entropy perturbation field.) The universe is like a linear amplifier in electronics: each harmonic component is modulated by an analog filter. Note that the transfer function depends on spatial frequency but not direction, because the equations of motion are rotationally invariant.

Using equations (70), (76), (77), and (78), plus the orthonormality of the spherical harmonics ($\int d\Omega\, Y_{lm}(\hat{k}) Y^*_{l'm'}(\hat{k}) = \delta_{ll'}\, \delta_{mm'}$), we get the key result for the angular power spectrum of the CMB:

$$C_l = 4\pi \int d^3k\, P_\phi(k) D_l^2(k)\ . \tag{79}$$

Here, $P_\phi(k)$ is the primeval power spectrum. For scale-invariant initial fluctuations, $P_\phi \propto k^{-3}$.

The dominant contribution to large-scale anisotropy is the Sachs-Wolfe effect, for which $D_l = C(\phi_e/\phi_i) j_l(k\chi_e)$. For a scale-invariant spectrum, equation (79) can be integrated exactly giving $C_l \propto 1/[l(l+1)]$, corresponding to equal power per logarithmic interval of angular degree l, i.e. a flat spectrum on the sphere. (In d dimensions, a scale-invariant spectrum is k^{-d}. For large l, the effective wavenumber is $k \propto l$.) This is why plots of the CMB power spectrum always show $l(l+1)C_l$.

We can go beyond the Sachs-Wolfe approximation by replacing equation (72) with the exact equation (16). Each field such as $\delta_\gamma(\vec{x}, \tau)$ is written as a Fourier integral with the Fourier components proportional to the initial gravitational potential through a transfer function, e.g. $\delta_\gamma(\vec{k}, \tau) = \delta_\gamma(k, \tau)\phi_i(\vec{k})$, a straightforward generalization of equation (56). Thus, we may generalize equation (72) to (Seljak & Zaldarriaga 1996; note the modified coefficient of δ_γ due to our different definition here)

$$\begin{aligned} D_l(k) &= \int_0^{\tau_0} d\chi\, \dot{\zeta}(\tau_0 - \chi) \left[\frac{1}{3}\delta_\gamma + \phi + u_\gamma \frac{\partial}{\partial \chi} + \frac{1}{2}\Pi_{ij} n^i n^j \right]_{\rm ret} j_l(k\chi) \\ &\quad + \int_0^{\tau_0} d\chi\, \zeta(\tau_0 - \chi)\, \frac{\partial}{\partial_\tau}(\phi + \psi)(k, \tau_0 - \chi)\ , \end{aligned} \tag{80}$$

where $\zeta(\tau) = \exp[-\tau_{\rm T}(\tau_0 - \tau)]$ is the "visibility function" of equation (15) and subscript ret means to evaluate the quantity in brackets at $(k, \tau = \tau_0 - \chi)$. The functions δ_γ, ϕ,

u_γ, etc., are all transfer functions, i.e. they are solutions to the equations of motion in Fourier space subject to the initial conditions $\phi(k) = 1$, $\sigma(k) = 0$.

The transfer functions may be computed directly in $\vec{k}$-space or by Fourier transformation of the plane-parallel Green's functions by equation (59). The publicly available CMBFAST code (Seljak & Zaldarriaga 1996) computes them directly in $\vec{k}$-space, while Bashinsky (2001) and Bashinsky & Bertschinger (2002) have computed them (in the fluid approximation) by transforming the Green's functions.

9 Numerical results

In Section 6 we derived approximate results for the CMB anisotropy on large scales in the Sachs-Wolfe approximation, equation (48). Later, in Section 7, we worked out the plane-parallel Green's function solutions in the two-fluid approximation. Section 8 showed how to compute the angular correlation function and angular power spectrum from these ingredients. Here we present results for the two-fluid approximation and compare with the exact computation by CMBFAST. The CMBFAST code includes three physical processes that are excluded by the two-fluid approximation: a full treatment of neutrinos; photon diffusion; and the polarization-dependence and anisotropic scattering contributions of Thomson scattering.

Figure 5 shows the angular correlation function on small scales ($\theta < 2°$). There are four notable phenomena. First, the curves all show a prominent dip. This feature is associated with the overlap of acoustic rings in the CMB photosphere. Recall that the spherical Green's functions correspond to acoustic waves expanding at the speed of sound. By the time of recombination, these waves reach a comoving distance of about $0.5\tau_{\rm rec}$ (Fig. 4). At the distance of recombination, $\tau_{\rm rec}$ (the diameter of the acoustic sphere) subtends an angle of about 1.2°. Bashinsky & Bertschinger (2002) show how the sharp feature occurring at this angle (thin curve in Fig. 5) arises from the singularities of δ_γ at the acoustic wavefronts. For angular separations less than this, sound waves are able to establish acoustic contact. For larger angular separations, the correlations reflect the correlations present in the unmodified inflationary spectrum. (Causal effects extend to about twice the acoustic length because the speed of sound is about half the speed of light.)

The second notable result from Figure 5 is that the two-fluid approximation with instantaneous recombination (thin curve) recovers much of the qualitative behavior of the CMBFAST result (thick curve) but underestimates the anisotropy on small scales. The main reason for this is that the Doppler contribution has been neglected here. Thus, the largest source of CMB anisotropy is accounted for by the intrinsic ($\frac{1}{3}\delta_\gamma$) and gravitational redshift contributions, but the Doppler contribution is appreciable on scales less than the acoustic length.

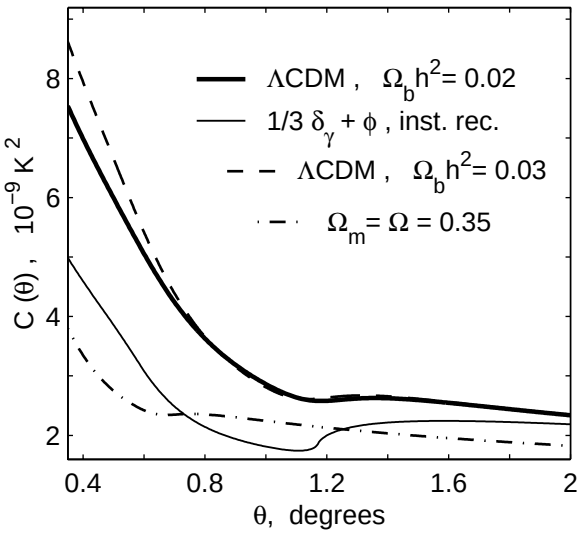

Figure 5: Angular CMB temperature correlation function. The parameters of the ΛCDM model are $\Omega_{\rm m} = 0.35$, $\Omega_\Lambda = 0.65$, $h = 0.65$ with a scale-invariant spectrum $P_\phi \propto k^{-3}$. For this set of parameters and the displayed $\Omega_{\rm b}h^2$ values, the acoustic sphere subtends an angle $\theta_s \simeq 1.2°$. The thin solid curve is calculated using the two-fluid approximation with instantaneous recombination. All the other curves are calculated using CMBFAST. The dip in $C(\theta)$ is shifted to smaller angles for the open model (dashed-dotted line). The slope for $\theta < \theta_s/2$ is dependent on the baryon density (dashed vs. solid line). Based on Bashinsky & Bertschinger (2001).

The third notable result is that the acoustic length in the open model (dashed-dotted curve in Fig. 5) subtends a smaller angle. This is simply because the angular distance $r(\chi)$ to the CMB photosphere is larger for an open model (Weinberg 2000).

Finally, Figure 5 shows that the baryon contribution has the most significant effect for angles less than half the diameter of the acoustic sphere. The baryon effect arises from the interplay between the wavefront singularity and the central valley in Figure 4. As we showed, the depth of that valley is proportional to Ω_b. This translates into a roughly linear dependence of the inner slope of $C(\theta)$ on Ω_b.

The angular correlation function has the attractive property of associating acoustic phenomena with localized features. The localization in angle means that a Fourier-Legendre representation will produce "ringing" (oscillations) in the angular frequency. Because the sphere is a compact manifold, the angular frequency l is discrete. Figure 6 plots the angular power spectrum C_l to show us that this ringing corresponds to the famous "acoustic peaks."

The fluid approximation yields surprisingly accurate prediction of the CMB anisotropy

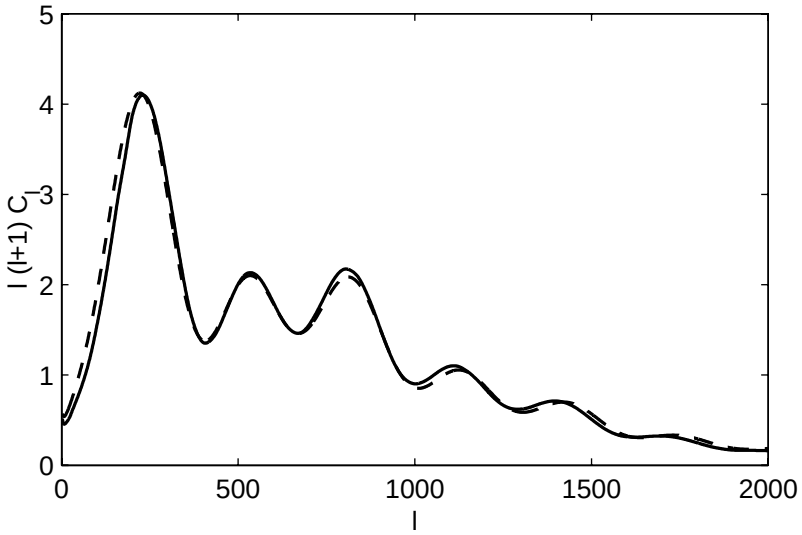

Figure 6: The angular power spectrum of CMB temperature anisotropy calculated using the two-fluid approximation (solid line, including the Doppler contribution) and using CMBFAST (dashed line). The ΛCDM model parameters are the same as for the thick solid curve in Fig. 5. From Bashinsky (2001).

spectrum. With a phenomenological correction for photon diffusion, the error of our numerical calculations in fluid approximation is within 5% on angular scales from 2π to a few arcminutes, see Fig. 9. It can also compute the gravitational radiation (tensor mode) and gravitational lensing (secondary) contributions to anisotropy.

The agreement between the two-fluid approximation and CMBFAST is much better in Figure 6 than in Figure 5. There are several reasons for this improvement. First, all the anisotropy contributions in equation (80) have now been included except for $\Pi_{ij}n^i n^j$ (polarization and anisotropic scattering terms). Second, photon diffusion was included approximately in a phenomenological manner. Third, recombination was gradual rather than instantaneous. Seljak (1994) included these effects in his earlier two-fluid treatment, however he did not include the integrated Sachs-Wolfe effect and he used the instantaneous recombination approximation, with some analytic corrections that are not as accurate as our numerical integrations. Our two-fluid model achieves accuracy better than 5% in C_l for $l \leq 1500$.

It appears that the approximate description given by equations (52) captures well the essential physics of the cosmological dynamics of the CMB photons and the other components with which they interact. Although CMBFAST remains the method of choice for accurate calculations and data analysis, the simplified model presented in

these notes provides a useful way to comprehend the dynamics of CMB anisotropy.

I would like to thank Sergei Bashinsky for his collaboration and for many helpful discussions, without which these notes would be impossible.

References

[1] Bardeen, J. M. 1980, PRD, 22, 1882.

[2] Bashinsky, S. 2001, MIT PhD thesis.

[3] Bashinsky, S., & Bertschinger, E. 2001, PRL, 87, 081301.

[4] Bashinsky, S., & Bertschinger, E. 2002, PRD, 65, 123008.

[5] Bertschinger, E. 1996, in *Cosmology and Large Scale Structure*, proc. Les Houches Summer School, Session LX, ed. R. Schaeffer, J. Silk, M. Spiro, and J. Zinn-Justin (Amsterdam: Elsevier Science), 273-347.

[6] Hu, W., Seljak, U., White, M., & Zaldarriaga, M. 1998, PRD, 57, 3290.

[7] Kodama, H., & Sasaki, M. 1984, Prog. Theor. Phys. Suppl., 78, 1.

[8] Kodama, H., & Sasaki, M. 1986, Int. J. Mod. Phys., A1, 265.

[9] Ma, C.-P., & Bertschinger, E. 1995, ApJ, 455, 7.

[10] Rees, M. J., & Sciama, D. W. 1968, Nature, 517, 611.

[11] Sachs, R. K., & Wolfe, A. M. 1967, ApJ, 147, 73.

[12] Seljak, U. 1994, ApJ, 435, L87.

[13] Seljak, U. 1996, ApJ, 463, 1.

[14] Seljak, U., & Zaldarriaga, M. 1996, ApJ, 469, 437.

[15] Spergel, D. N., & Zaldarriaga, M. 1997, PRL, 79, 2180.

[16] Weinberg, S. 2000, PRD, 62, 127302.

[17] Weinberg, S. 2002, astro-ph/0207375.

[18] Zaldarriaga, M., & Seljak, U. 1997, PRD, 55, 1830.

[19] Zaldarriaga, M., Seljak, U., & Bertschinger, E. 1998, ApJ, 494, 491.